LAMELIS 2016
Lasers in Medicine and Life Sciences
Advanced summer school for students of medicine and physics
30th June – 9th July 2016

TOTAL INTERNAL REFLECTION FLUORESCENCE MICROSCOPY

principles & applications

Beáta Bugyi

UNIVERSITY OF PÉCS – MEDICAL SCHOOL – DEPARTMENT OF BIOPHYSICS
CYTOSKELETAL DYNAMICS LAB
http://cytoskeletaldynamics.wix.com/mysite

OUTLINE

CLASSICAL RESOLUTION LIMIT OF THE LIGHT MICROSCOPE

TOTAL INTERNAL REFLECTION FLUORESCENCE MICROSCOPY

- HISTORICAL PERSPECTIVES
- PHYSICAL PRINCIPLES
- TECHNICAL CONSIDERATIONS

APPLICATIONS

- PROTEIN BIOCHEMISTRY APPLICATION
- MICROPATTERING-BASED BIOMIMETIC APPLICATIONS
- CELL BIOLOGY APPLICATIONS
- SINGLE MOLECULE LOCALIZATION

CLASSICAL LIMIT OF RESOLUTION

1873 DIFFRACTION LIMIT THEORY
(Ernst Abbe, Carl Zeiss)

RESOLUTION IS INTRINSICALLY LIMITED BY THE WAVE NATURE OF LIGHT.

$$(d_x, d_y) = \Delta = 0.61\frac{\lambda}{NA} \sim 200\ nm$$

$$d_z = 2n\frac{\lambda}{(NA)^2} \sim 800\ nm$$

$$NA = n\sin\alpha$$

OBJECT (POINT) → IMAGE (3D STRUCTURE)

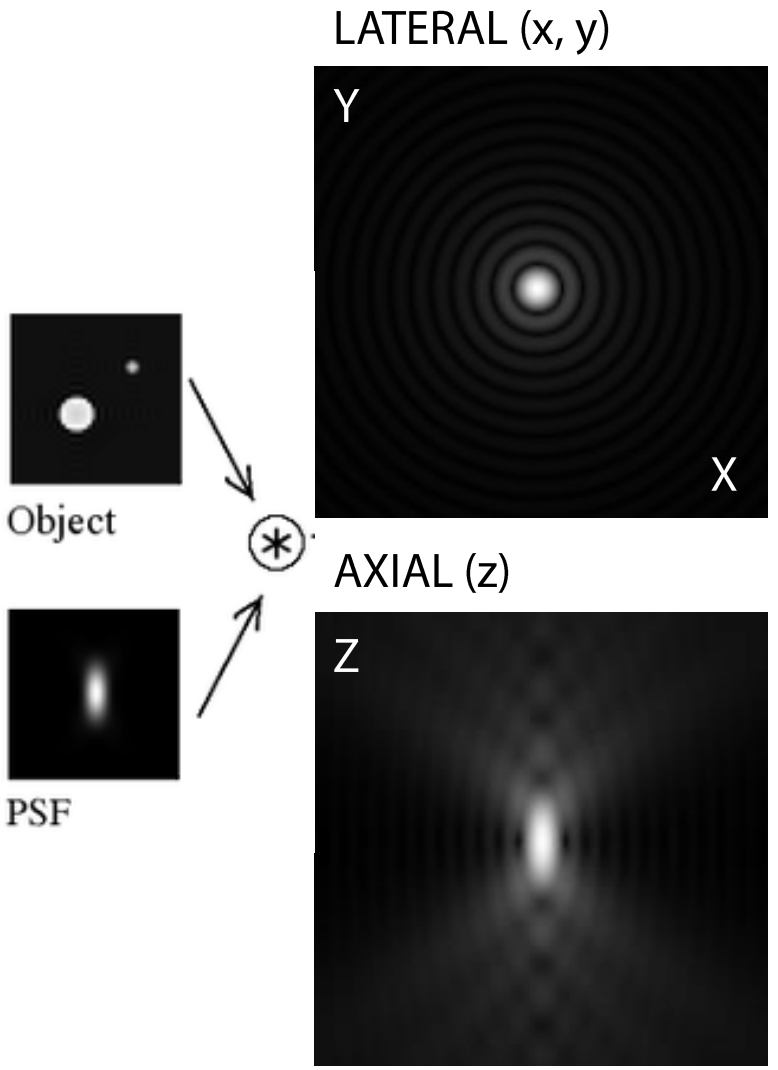

„SUPER-RESOLUTION" FLUORESCENCE MICROSCOPY

FLUORESCENCE MICROSCOPE (1911)
CONFOCAL MICROSCOPY (1961)

- illumination through pinhole (~500 – 600 nm)

Minsky, M. Microscopy Apparatus. US Patent 3,013,467 (1961)

TOTAL INTERNAL REFLECTION FLUORESCENCE MICROSCOPY (1981)

- evanescent wave illumination (~ 100 nm)

Axelrod, D. Cell-substrate contacts illuminated by total internal reflection fluorescence. J. Cell Biol. 89, 141–145 (1981)

STIMULATED EMISSION MICROSCOPY (2000)

- PSF engineering, stimulated emission of fluorescence (~ tens of nm)

Klar, T. A., Jakobs, S., Dyba, M., Egner, A. & **Hell, Stefan.** W. Fluorescence microscopy with diffraction resolution barrier broken by stimulated emission. *Proc. Natl Acad. Sci. USA* **97**, 8206–8210 (2000)

SINGLE MOLECULE LOCALIZATION MICROSCOPY (STORM, PALM) (2006)

- phototransformable fluorophores, Gaussian fit (~ tens of nm)

Betzig, Eric. *et al.* Imaging intracellular fluorescent proteins at nanometer resolution. *Science* **313**, 1642–1645 (2006)
Rust, M. J., Bates, M. & Zhuang, X. Sub-diffractionlimit imaging by stochastic optical reconstruction microscopy (STORM). *Nature Methods* **3**, 793–796 (2006)
Dickson RM, Cubitt AB, Tsien RY and **Moerner William** (1997) On/off blinking and switching behaviour of single molecules of green fluorescent protein. Nature 388:355-358.

STRUCTURED ILLUMINATION MICROSCOPY (2008)

- sequential illumination through a rotating grid (~ 100 nm)

Karadaglic, D. and Wilson, T. Image formation in structured illumination wide-field fluorescence microscopy. Micron 39: 808-818 (2008).

TOTAL INTERNAL REFLECTION MICROSCOPY

E. J. Ambrose
Nature 1956

„In order to study the contacts formed between cells and solid surfaces, it is possible to make use of the **slight penetration of light waves into the less dense medium when totally internally reflected** at the glass/water interface."

nonfluorescent, evanescent light scattering from cells

crease with duration of the heating, the radioactive yield into purified *p*-nitro benzoic acid is likely to be much less than 44 per cent in the second case.

After purification, and removal of the activity from the carboxyl group, the overall yield was about 70 per cent by weight (17 per cent by activity), the specific activity being 230 mc./gm.

Further studies on the use of this material are in progress. A detailed account of the method will be published elsewhere.

J. E. S. Bradley

Physics Department,
Middlesex Hospital Medical School,
London, W.1.
Sept. 7.

[1] Ingold, C. K., Raisin, C. G., and Wilson, C. L., *Nature*, **134**, 734 (1934).
[2] Best, A. P., and Wilson, C. L., *J. Chem. Soc.*, 239 (1946).
[3] Gold, V., and Satchell, D. P. N., *J. Chem. Soc.*, 3609 (1955).
[4] Gold, V., and Satchell, D. P. N., *J. Chem. Soc.*, 3622 (1955).
[5] Koizumi, M., and Titani, T., *Bull. Chem. Soc. Japan*, **13**, 318 (1938).

A Surface Contact Microscope for the study of Cell Movements

The importance of the contacts formed by moving cells in controlling their behaviour has been clearly shown in the phenomenon of contact guidance described by Weiss[1] and in contact inhibition described by Abercrombie and Heaysman[2].

In order to study the contacts formed between cells and solid surfaces, it is possible to make use of the slight penetration of light waves into the less dense medium when totally internally reflected at a glass/water interface. The apparatus used for these studies is illustrated in Fig. 1. Light from an intense source *S* (compact-source mercury arc) passes through the slit *T* and strikes the upper surface *A* of the 60°-prism. A cell suspension in water is mounted between an ordinary microscope slide and a coverslip and is sealed with immersion oil on the upper face of the prism (Fig. 2). The incident light now strikes the upper surface of the glass slide at an angle greater than the critical angle and is totally internally reflected at the glass/water interface. In reality the beam penetrates the less dense medium slightly, as shown diagrammatically in Fig. 3(*a*). If a cell of refractive index greater than water is moving on

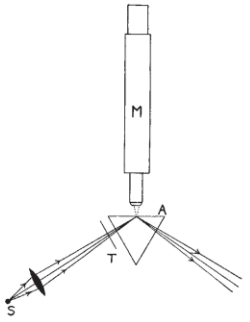

Fig. 1

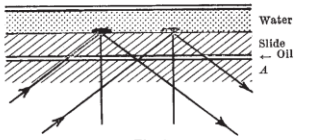

Fig. 2

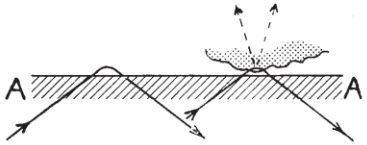

Fig. 3

the surface (Fig. 3(*b*)), those portions which make close contact with the surface of the glass will enter the penetrating beam and will scatter the light, owing to the presence of minute inhomogeneities in their structure.

When seen from above, through the microscope *M*, the field appears completely dark, provided that the incident light beam has been carefully shielded and the prism faces are clean. But those regions of the moving cells which are in close contact with the glass are brightly illuminated. In addition, the actual contours of the cell surface can be explored by changing the angle of the incident beam. With increasing angle, the degree of penetration of the incident beam is decreased so that the areas of the cell which are illuminated are reduced, eventually to those regions which are almost in molecular contact with the glass surface.

The effect is particularly well illustrated in the case of a filamentous mould kindly provided by Dr. R. J. Goldacre. As the mould moves forward along the glass, bright waves of light can be seen to move rapidly along its length, which are due to continuous changes in the points of adhesion between the lower surface of the mould and the glass surface. Apart from its biological application, the microscope may prove to be generally useful for the study of a number of phenomena, particularly those connected with the forces of cohesion between surfaces.

I am grateful to Prof. A. Haddow for his interest and encouragement in this work. This investigation has been supported by grants to the Chester Beatty Research Institute (Institute of Cancer Research: Royal Cancer Hospital) from the British Empire Cancer Campaign, Jane Coffin Childs Memorial Fund for Medical Research, the Anna Fuller Fund and the National Cancer Institute of the National Institutes of Health, U.S. Public Health Service.

E. J. Ambrose

Chester Beatty Research Institute,
Institute of Cancer Research:
Royal Cancer Hospital,
London, S.W.3.
July 27.

[1] Weiss, P., "Principles of Development" (Henry Holt and Co., New York, 1939).
[2] Abercrombie, M., and Heaysman, J. E. M., *Exp. Cell Res.*, **5**, 111 (1953); **6**, 293 (1954).

http://www.nature.com/nature/journal/v178/n4543/abs/1781194a0.html

TOTAL INTERNAL REFLECTION FLUORESCENCE MICROSCOPY

D. Axelrod
Journal of Cell Biology 1981

„The new method is an application … and extension to fluorescence of the total internal reflection micorscope illumination system introduced by Ambrose."

Cell-Substrate Contacts Illuminated by Total Internal Reflection Fluorescence

DANIEL AXELROD
Biophysics Research Division and Department of Physics, University of Michigan, Ann Arbor, Michigan 48109

ABSTRACT A technique for exciting fluorescence exclusively from regions of contact between cultured cells and the substrate is presented. The technique utilizes the evanescent wave of a totally internally reflecting laser beam to excite only those fluorescent molecules within one light wavelength or less of the substrate surface. Demonstrations of this technique are given for two types of cell cultures: rat primary myotubes with acetylcholine receptors labeled by fluorescent α-bungarotoxin and human skin fibroblasts labeled by a fluorescent lipid probe. Total internal reflection fluorescence examination of cells appears to have promising applications, including visualization of the membrane and underlying cytoplasmic structures at cell-substrate contacts, dramatic reduction of autofluorescence from debris and thick cells, mapping of membrane topography, and visualization of reversibly bound fluorescent ligands at membrane receptors.

The regions of contact between a tissue culture cell and a solid substrate are of considerable interest in cell biology. These regions are obvious anchors for cell motility (1), loci for aggregation of specific membrane proteins (2–4), and convergence points for cytoskeletal filaments (2, 5, 6). Described here is a fluorescence microscope method for selectively visualizing specific molecules in cell-substrate contact regions while avoiding fluorescence excitation of the cell interior liquid medium and cellular debris. Other potential applications of this method include viewing fluorescence-marked receptors at very low cell surface concentrations, cytoplasmic filaments in thick cells, and fluorescent agonists that bind reversibly to the cell membrane.

The new method is an application of total internal reflection fluorescence (TIRF) to cellular microscopy and is an extension to fluorescence of the total internal reflection microscope illumination system introduced by Ambrose (7) to detect light scattered at cell-substrate contacts. TIRF microscopy utilizes a light beam in the substrate that is obliquely incident upon the substrate liquid interface at an angle greater than the critical angle of refraction. At this angle, the light beam is totally reflected by the interface. However, an electromagnetic field called the "evanescent wave" does penetrate into the liquid medium. The evanescent wave propagates parallel to the surface with an intensity I that decays exponentially with perpendicular distance z from the surface:

$$I = I_o \exp(-z/d) \quad (1)$$

The characteristic exponential decay depth d is:

$$d = \frac{\lambda}{4\pi n_2}\left(\frac{\sin^2\theta}{\sin^2\theta_c} - 1\right)^{-1/2}, \quad (2)$$

where n_1 = refractive index of the substrate; n_2 = refractive index of the liquid medium; θ_c = the critical angle of incidence $= \sin^{-1} n_2/n_1$; θ = the angle of incidence, $\theta > \theta_c$; and λ = the wavelength of incident light in vacuum. The decay depth d decreases with increasing θ. Except for θ close to θ_c (where $d \to \infty$), d is on the order of λ or smaller. I_o, the intensity of the evanescent wave at $z = 0$, is on the order of the incident light intensity except for angles of incidence very near the critical angle (8). Therefore, for most experimental configurations, a fluorescent molecule located in the evanescent wave at $z = 0$ will be excited with roughly the same efficiency as it would if it were located in the incident beam.

A fluorescent molecule located close to the surface in the evanescent wave can become excited and emit fluorescence; molecules much farther away will not be excited. The efficiency of excitation decays exponentially according to Eqs. 1 and 2. For typical experiments described here, identical fluorescent molecules located at 1, 10, 100, and 1,000 nm from the surface will emit relative fluorescence intensities of 0.99, 0.92, 0.43, and 0.0002, respectively. For cells adhering to the surface, only fluorescent molecules at or near the cell surface in the regions of closest contact with the substrate will be excited significantly.

TIRF has been employed previously to study surface interactions in a variety of molecular systems, including solutions of fluorescein (9) and serum albumin (10, 11) at glass surfaces, and antibodies at antigen coated surfaces (12). More recently, TIRF has been combined with fluorescence photobleaching recovery and fluorescence correlation spectroscopy to study the surface adsorption/desorption kinetics of fluorescent macromolecules (13, 14) and viruses (15).

A completely unrelated transmitted illumination technique,

THE JOURNAL OF CELL BIOLOGY · VOLUME 89 APRIL 1981 141-145

PHYSICAL PRINCIPLES OF TIRFM

TOTAL INTERNAL REFLECTION – CRITICAL ANGLE

SNELL'S LAW OF REFRACTION

$$n_1 sin\alpha_1 = n_2 sin\alpha_2$$

IF

$$\boldsymbol{n_1 > n_2}$$

THEN

$$\alpha_1 < \alpha_2$$

CRITICAL ANGLE

$\alpha_{critical} \equiv \alpha_1$ when $\alpha_2 = 90^0$

$$\boldsymbol{\frac{n_1}{n_2} sin\alpha_{critical} = 1}$$

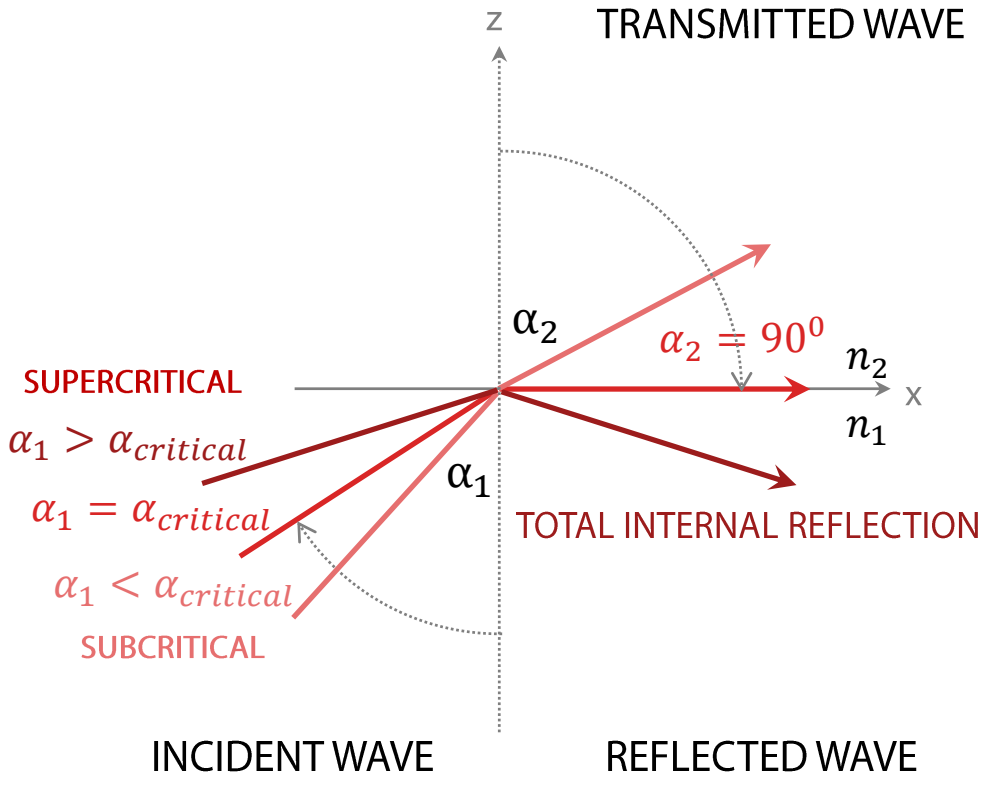

Notation:
1: incident wave/1st medium
2: transmitted wave/2nd medium

TOTAL INTERNAL REFLECTION – CRITICAL ANGLE

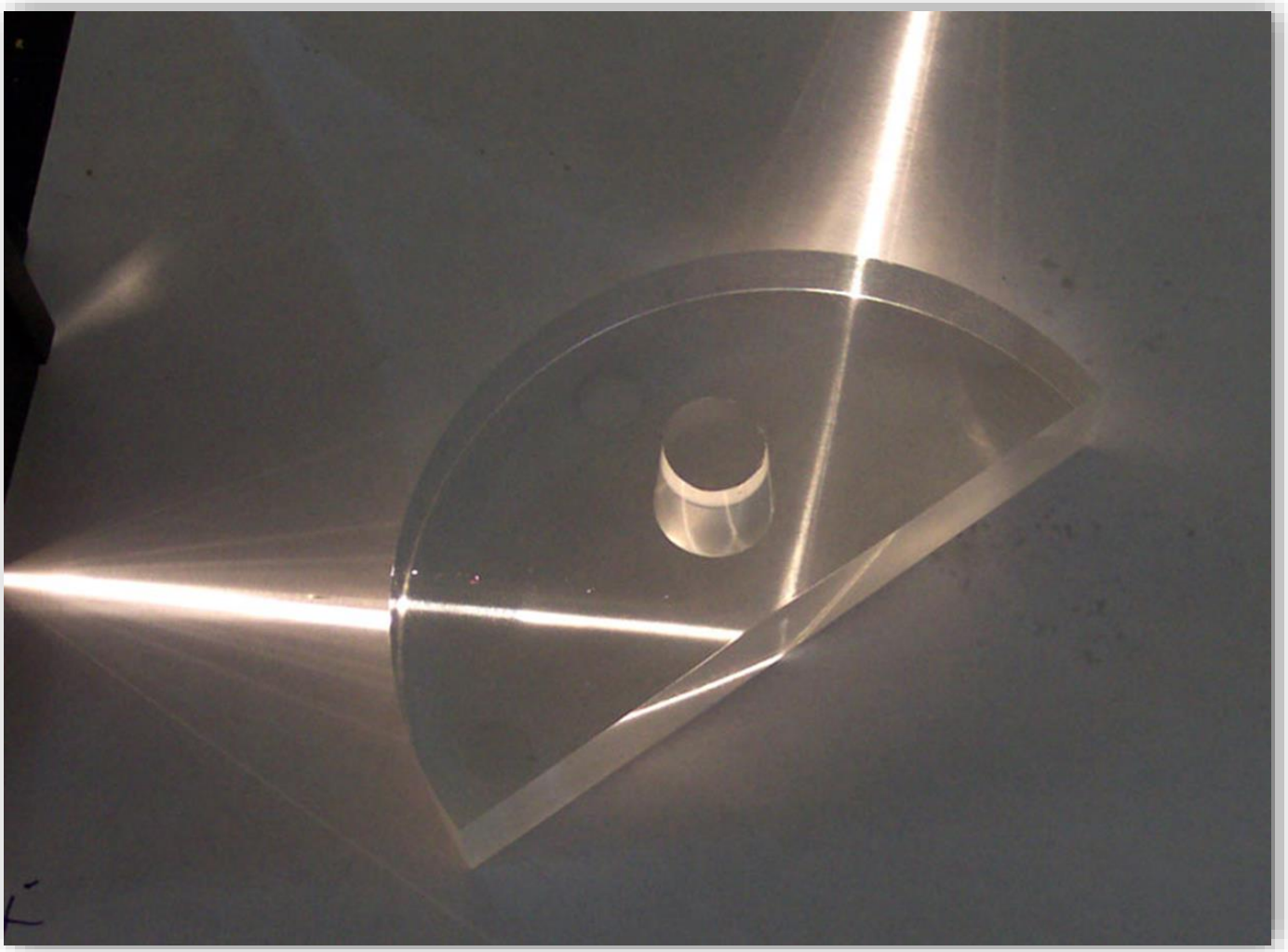

TOTAL INTERNAL REFLECTION – EVANESCENT WAVE

EVANESCENT WAVE

MONOCHROMATIC PLANE WAVE

INCIDENT

$$\vec{E}_1(\vec{r},t) = \vec{E}_1 \exp\left[i(\vec{k}_1\vec{r} - \omega t)\right]$$

TRANSMITTED

$$\vec{\mathbf{E}}_2(\vec{\mathbf{r}},\mathbf{t}) = \vec{\mathbf{E}}_2 \mathbf{exp}\left[\mathbf{i}\left(\vec{\mathbf{k}}_2\vec{\mathbf{r}} - \boldsymbol{\omega}\mathbf{t}\right)\right] =$$
$$= \vec{E}_2 \exp\left[i(k_2 sin\alpha_2 x + k_2 cos\alpha_2 z - \omega t)\right]$$

$$ik_2(sin\alpha_2 x + cos\alpha_2 z) = ik_2\left(\frac{sin\alpha_1}{n}x + i\sqrt{\frac{sin^2\alpha_1}{n^2} - 1}z\right)$$

IF $\alpha_1 = \alpha_c$, then $\vec{\mathbf{E}}_2(\vec{\mathbf{r}},\mathbf{t}) =$

$$= \vec{E}_2 exp[i(k_2 x - \omega t)]$$

IF $\alpha_1 > \alpha_c$, then $\vec{E}_2(\vec{r},t) =$

$$= \vec{E}_2\, exp\left[i\left(k_2 \frac{sin\alpha_1}{n}x - \omega t\right)\right] \cdot exp\left[-k_2\sqrt{\frac{sin^2\alpha_1}{n^2} - 1}z\right]$$

The transmitted wave propagates parallel to the surface (x axis), as well as in the z direction, where it is attenuated exponentially.

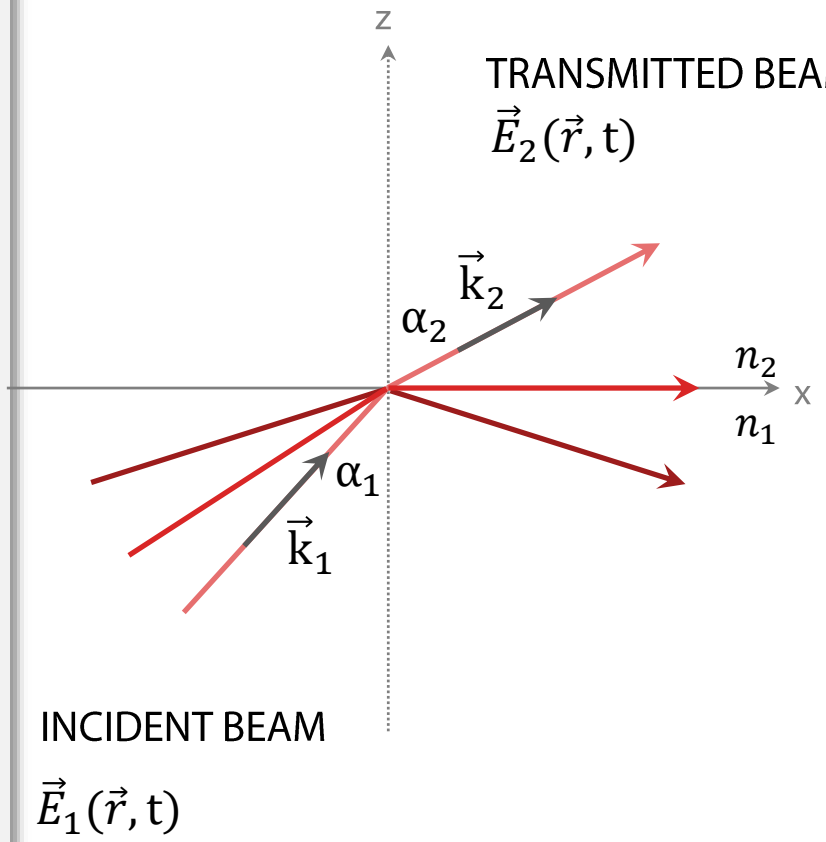

TOTAL INTERNAL REFLECTION – EVANESCENT WAVE

EVANESCENT WAVE

$$\vec{E}_{\text{evanescent}}(\vec{r}, t) =$$

$$\vec{E} exp[-k_2 \sqrt{\frac{sin^2\alpha_1}{n^2} - 1} z]$$

$$= \vec{E} exp\left[-\frac{2\pi}{\lambda}\frac{1}{n_2}\sqrt{sin^2\alpha_1 {n_1}^2 - {n_2}^2} z\right]$$

INTENSITY PROFILE

$$I(z) = \left|\vec{E}\right|^2 = \mathbf{I_0 exp}\left(-\frac{\mathbf{z}}{\mathbf{d}}\right)$$

WHERE

$$\mathbf{d} = \frac{\boldsymbol{\lambda}}{\mathbf{4\pi n_1}}(\mathbf{sin^2\alpha_1} - (\frac{\mathbf{n_2}}{\mathbf{n_1}})^2)^{-\frac{1}{2}}$$

PENETRATION DEPTH/DECAY LENGTH

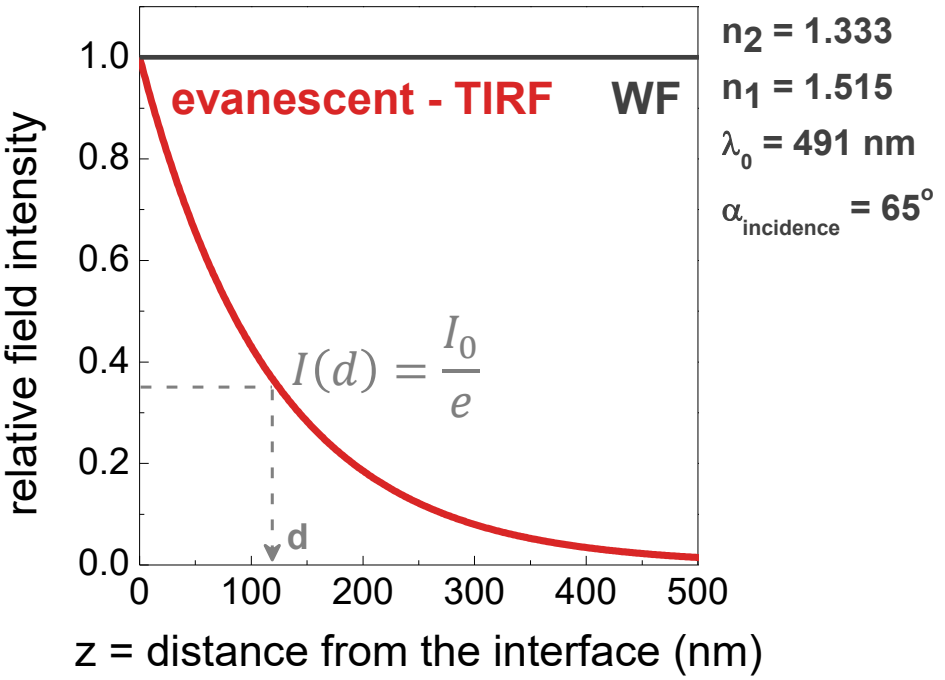

TOTAL INTERNAL REFLECTION – CRITICAL ANGLE

CRITICAL ANGLE

$$sin\alpha_{critical} = \frac{n_2}{n_1}$$

$\alpha_{critical}$ depends on the relative refractive index ratio of the two media. If the $n = n_2/n_1$ is small, the critical angle is shallow and TIR is easily achieved.

GLASS : WATER INTERFACE

$$\frac{n_2}{n_1} = 0.879$$

$$\alpha_{critical} = 61.62^o$$

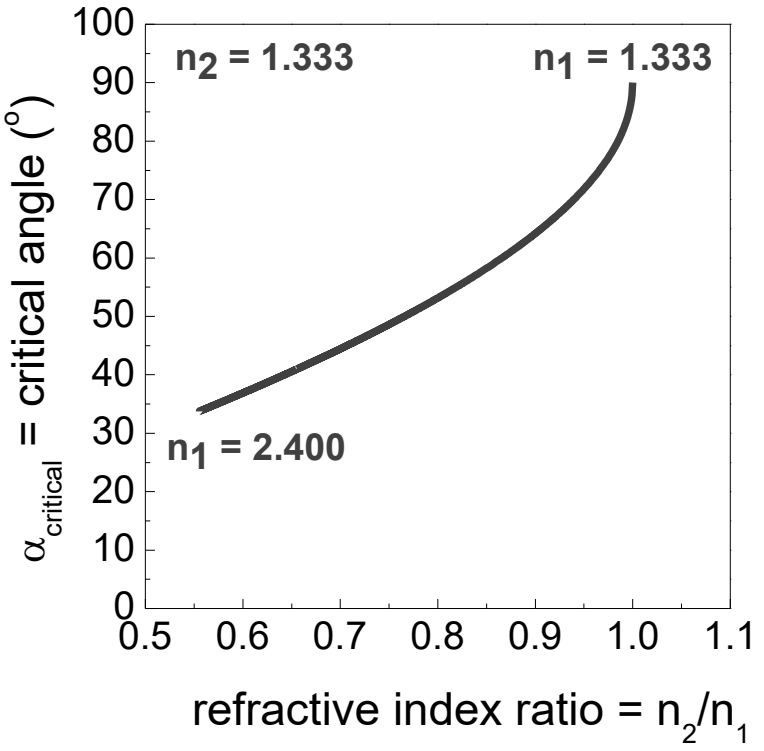

INFLUENCES ON THE „EVANESCENT" NATURE

$$d = \frac{\lambda}{4\pi n_1}\left(\sin^2\alpha_1 - \left(\frac{n_2}{n_1}\right)^2\right)^{-\frac{1}{2}}$$

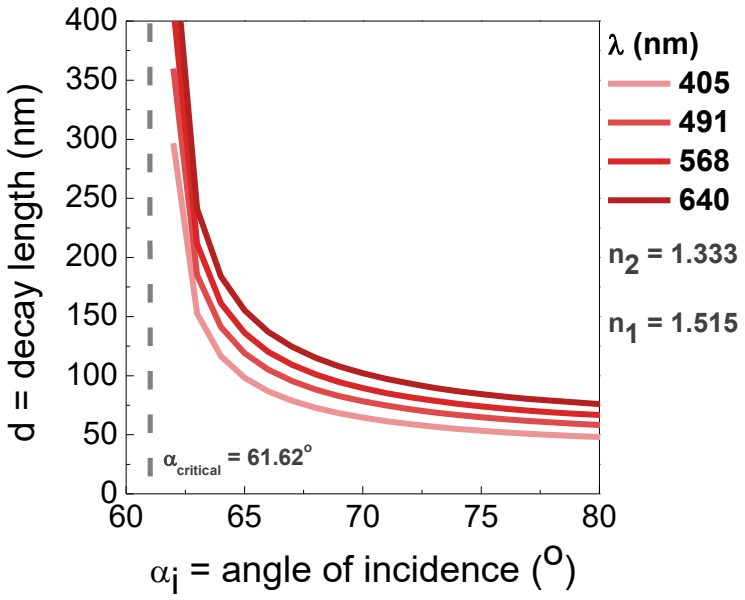

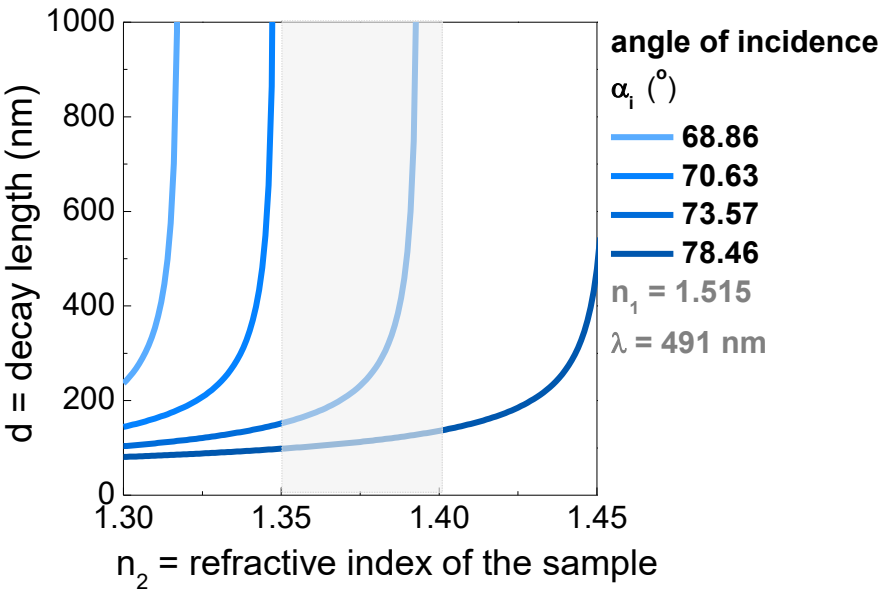

As the angle of incidence increases, the depth becomes narrower (resolution!)

$$\boldsymbol{\alpha_1 \rightarrow \alpha_{critical}}\text{: } \boldsymbol{d \rightarrow \infty}$$

As the wavelength increases, the depth is narrower (resolution!)

As n_2 increases, the depth increases (resolution!).

As the angle of incidence increases, the sensitivity of the evanescent field to n_2 decreases.

TIRFM – EVANESCENT WAVE ILLUMINATION

TIRFM – EVANESCENT WAVE ILLUMINATION

- **EVANESCENT WAVE**
  - decays exponentially in intensity with increasing distance normal to the surface
  - decay length (d) is in the order of the wavelength of the incident light (λ)
  - selectively excite fluorophores very near a solid surface (~ 100 nm)
  - eliminates background fluorescence from out-of-focus planes, improves contrast

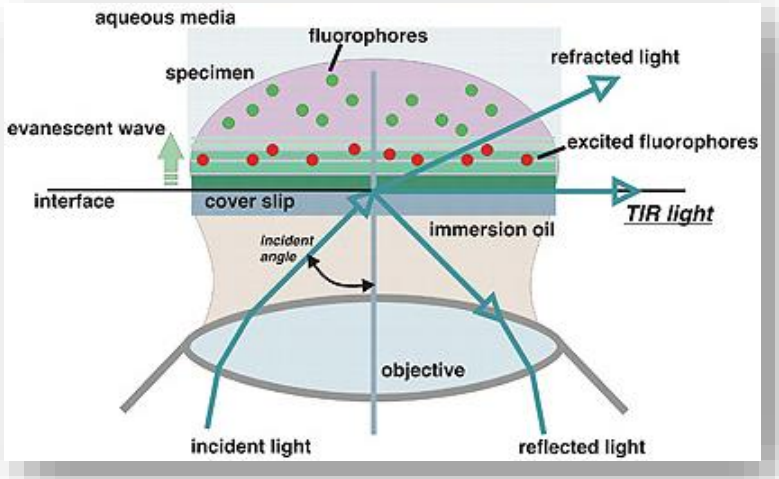

TIRFM, AS A NEAR-FIELD IMAGING METHOD PROVIDES A SURFACE-SELECTIVE ILLUMINATION AND RESOLUTION IMPROVEMENT DUE TO THE UNIQUE PROPERTIES OF THE EVANESCENT FIELD.

WF vs TIRF ILLUMINATION

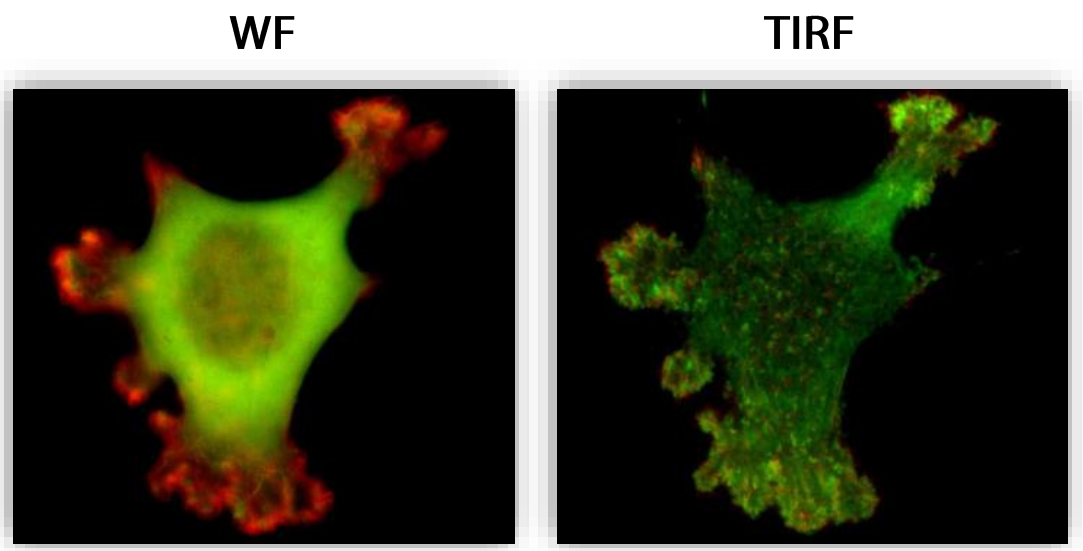

B16/F1 melanoma cell

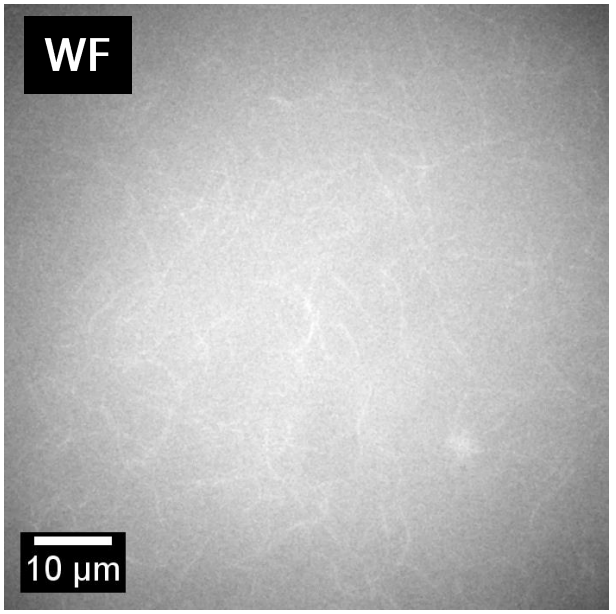

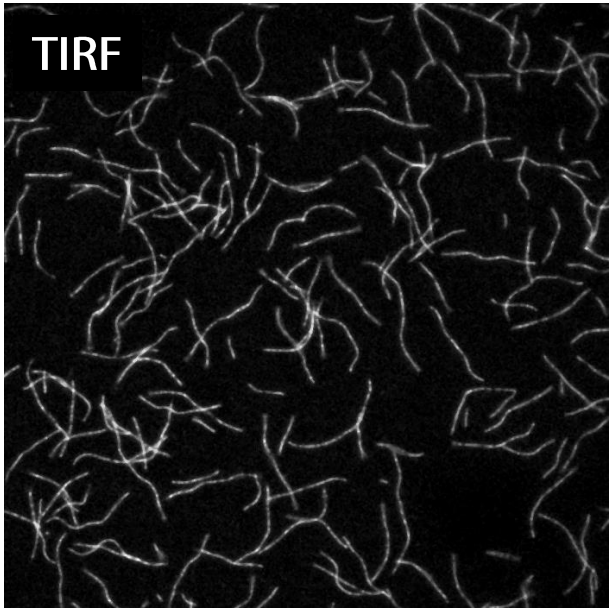

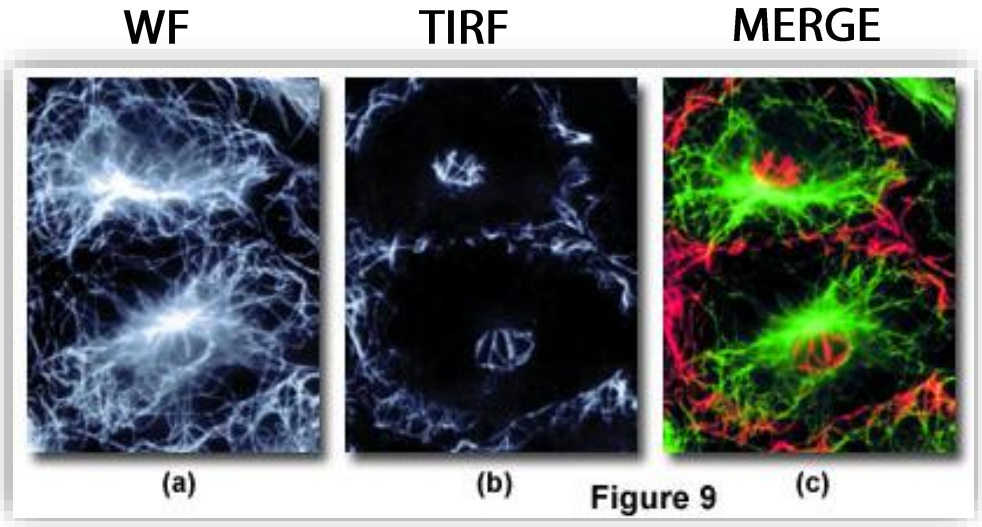

TRANSITION FROM WF TO TIRF

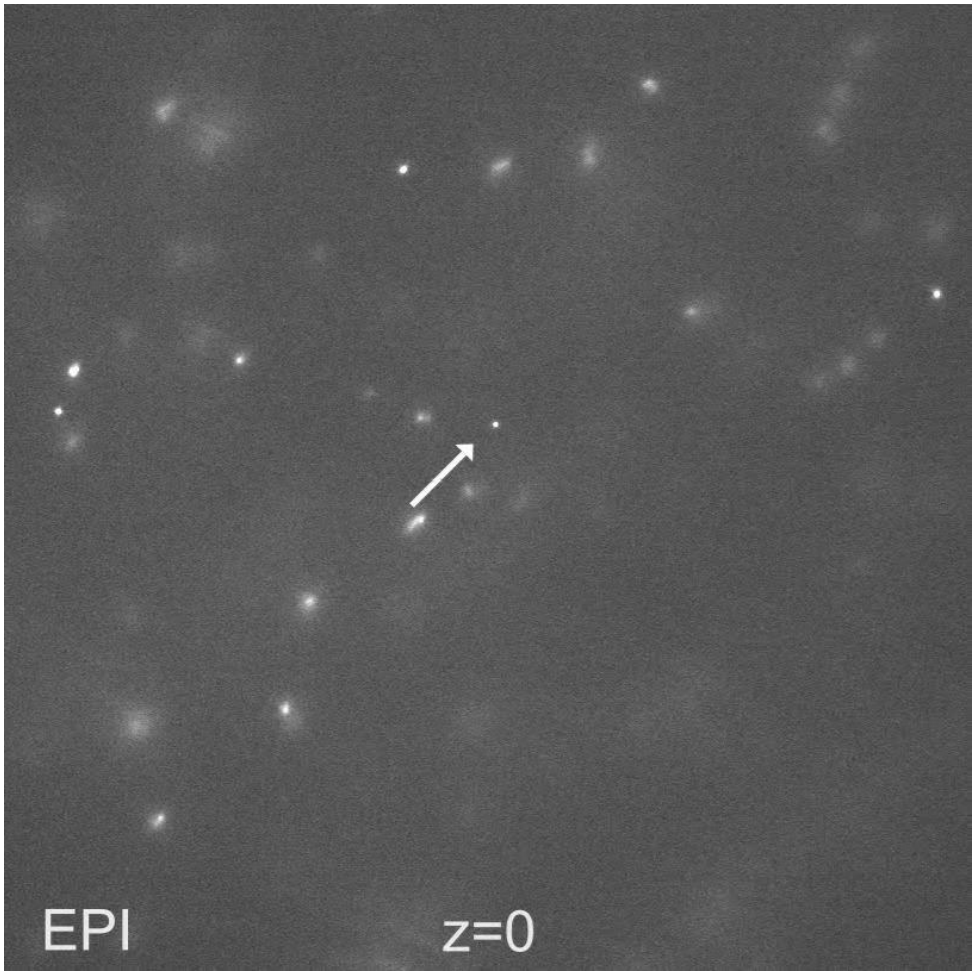

http://jcs.biologists.org/content/suppl/2010/10/19/123.21.3621.DC1

λ_{ex} = 491 nm, 60× 1.49 NA

TIRFM APPLICATIONS

- **EXTRACELLULAR MATRIX STRUCTURE AND ASSEMBLY**
- **CELL-SURFACE CONTACT REGIONS**
  - focal adhesion dynamics
- **CELL MEMBRANE, CELL SURFACE RECEPTORS, ION CHANNELS**
- **EXOCYTOSIS, SECRETORY VESICLE TRACKING**
- **ENDOCYTOSIS**
- **SUBMEMBRANE CYTOSKELETAL DYNAMICS**
  - actin, micortubule cytoskeleton

TIRFM + COMBINED ADVANTAGES

- FRAP
- FRET
- AFM
- SINGLE MOLECULE LOCALIZATION TECHNIQUES (STORM, PALM)
- MICORPATTERNING
- MICORFLUIDCS

TECHNICAL CONSIDERATIONS

HOW TO IMPLEMENT TIR PRINCIPLES INTO THE FLUORESCENCE MICROSCOPE?

- THE REFRACTIVE INDEX OF THE 2ND MEDIUM HAS TO BE LOWER THAN THAT OF THE 1ST ONE

$n_1 > n_2$

$n_{water(2)} = 1.333, n_{cell(2)} = 1.36$

$n_{glass(1)} = 1.515$

$n = \frac{n_2}{n_1} = 0.879, n = \frac{n_2}{n_1} = 0.898$

- **CRITICAL ANGLE OF ILLUMINATION**

THE ANGLE OF INCIDENCE HAS TO BE LARGER THAN THE CRITICAL ANGLE

$\alpha_{incidence} > \alpha_{critical}$

for glass : water interface: $\alpha_{critical} = 61.62^o$

for glass : cell interface: $\alpha_{critical} = 63.86^o$

TIRFM SETUP

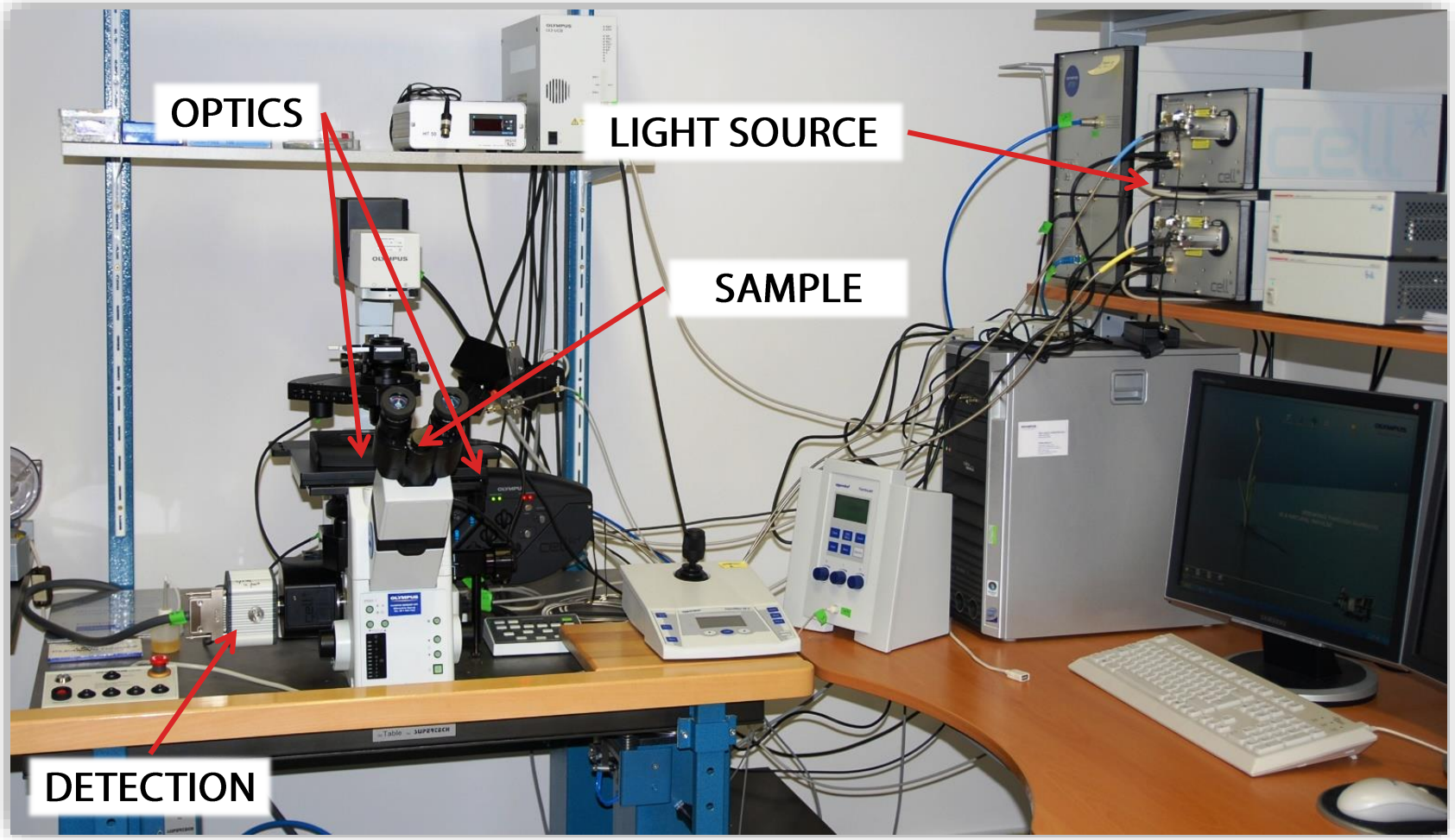

ARC LAMP-BASED ILLUMINATION

LAMP-BASED ILLUMINATION

DISCARD SUBCRITICAL ILLUMINATION

\+ EASY SELECTION OF EXCITATION WAVELENGTH

\- LOWER EXCITATION INTENSITY

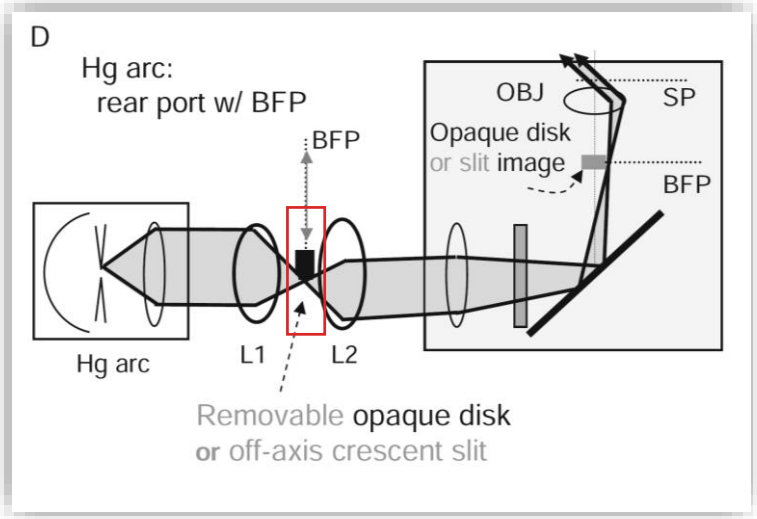

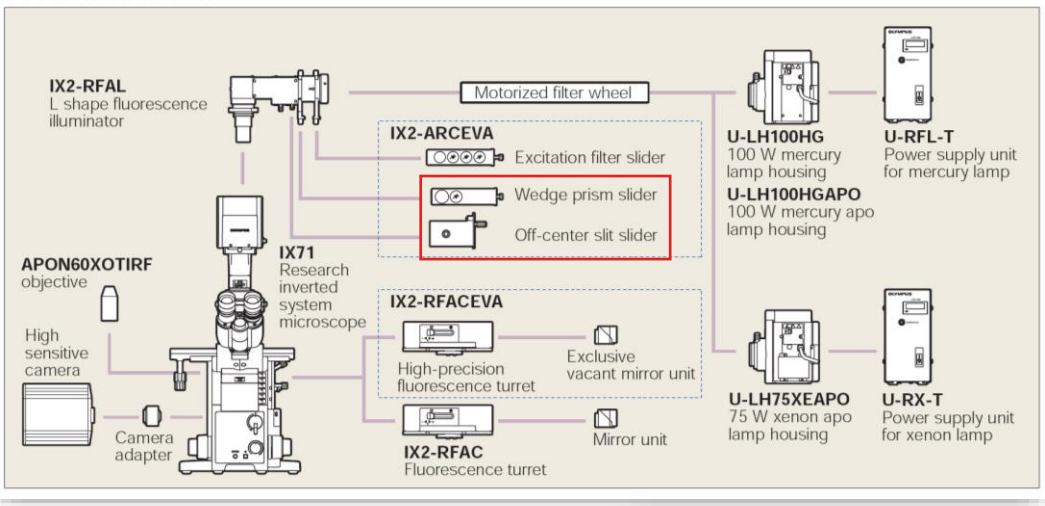

WEDGE PRISM

- circular prisms positioned at slight angles with respect to each other
- deflect light by reflection

http://www.olympusmicro.com/primer/java/prismsandbeamsplitters/wedgeprisms/

LASER-BASED ILLUMINATION

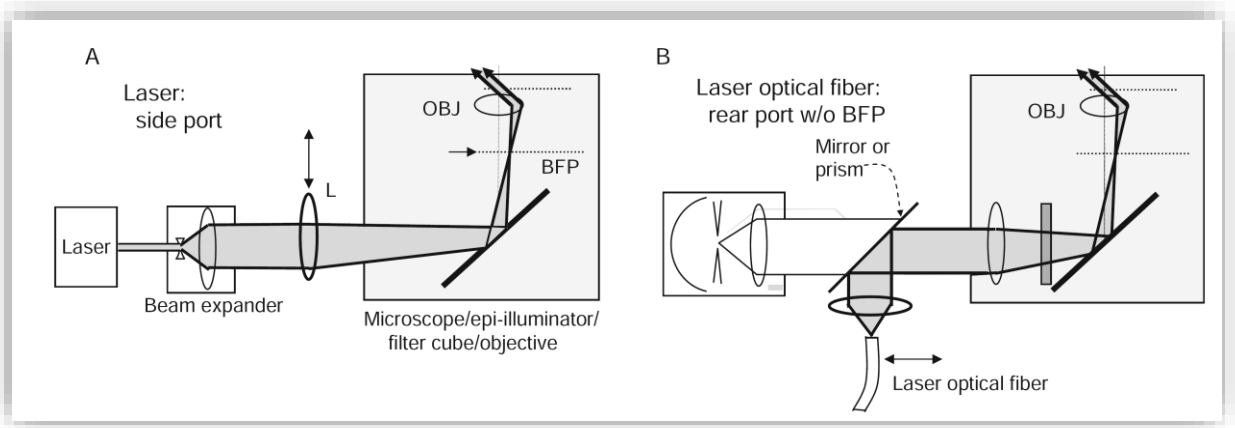

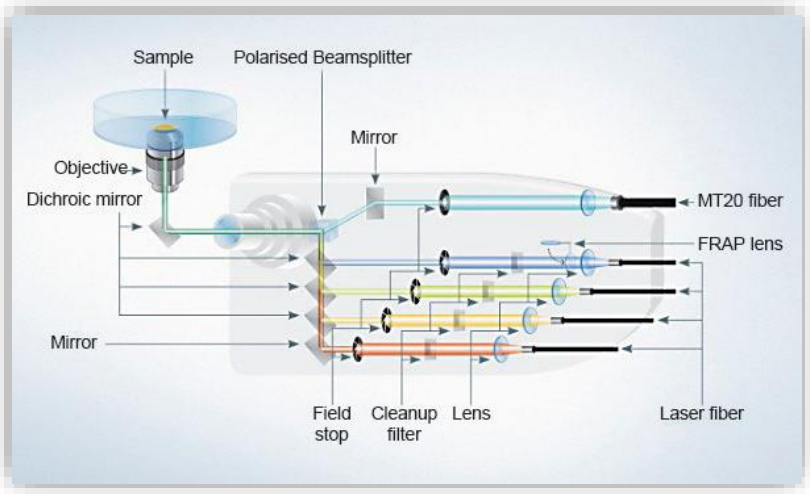

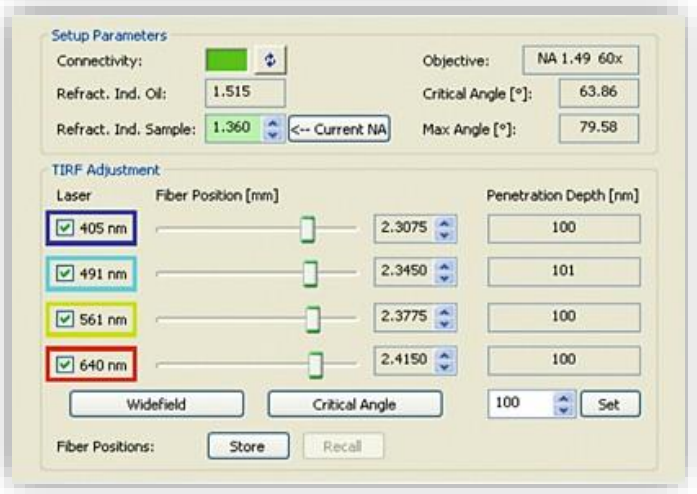

LASER

- DIODE LASER
- DIODE PUMPED SOLID STATE LASER
- P up to 300 mW
- λ = 405 - 640 nm

PRISM-BASED TIRFM

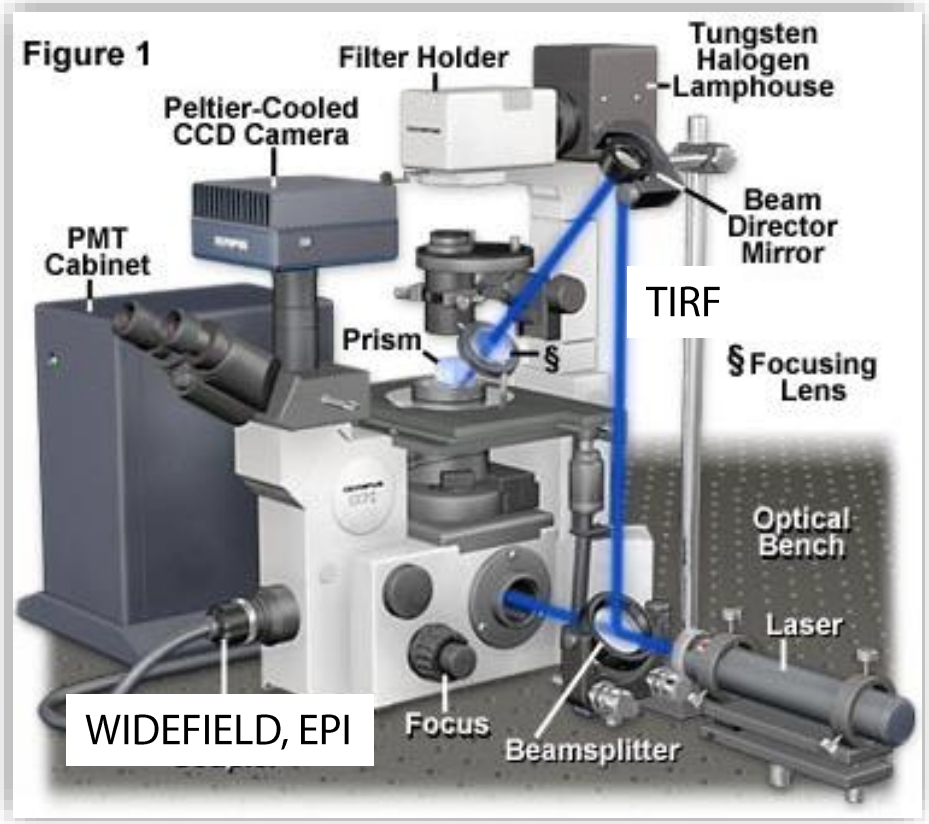

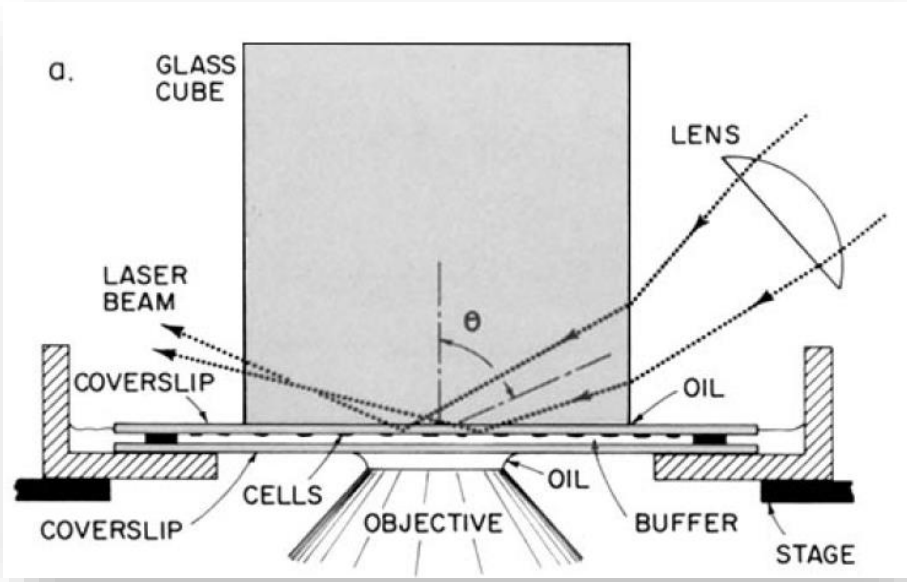

D. Axelrod Journal of Cell Biology 1981
http://www.olympusmicro.com/primer/techniques/fluorescence/tirf/tirfconfiguration.html

OBJECTIVE-BASED (PRISMLESS) TIRFM

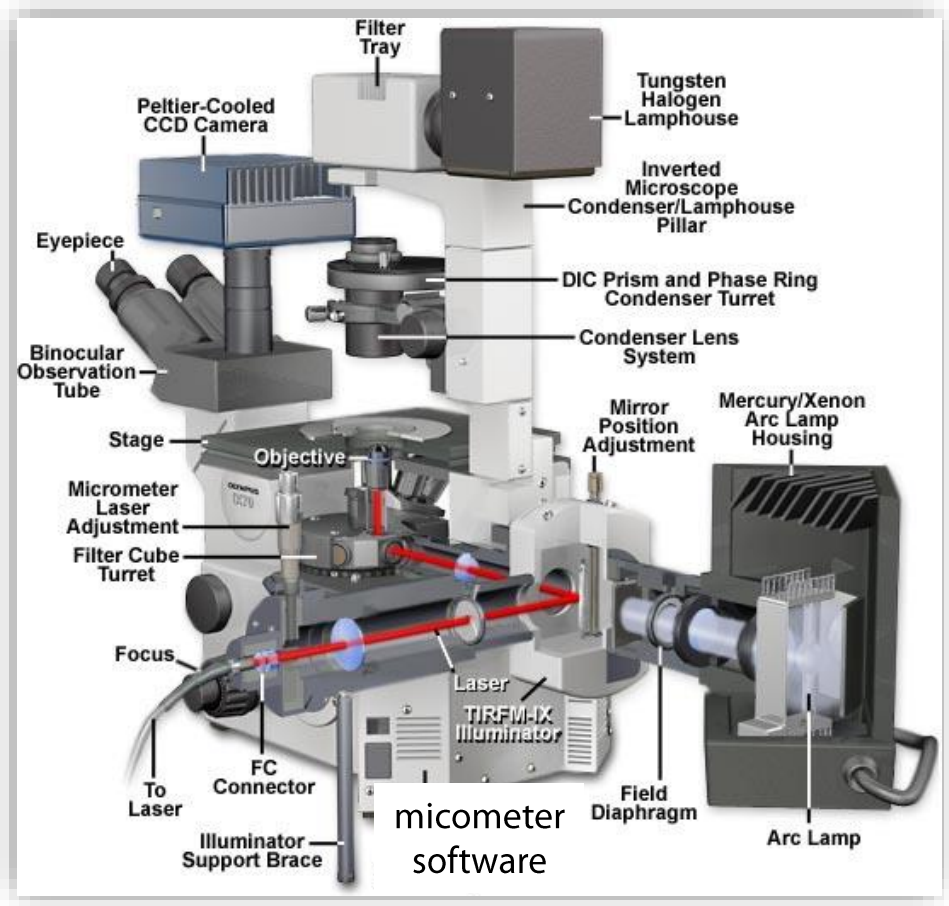

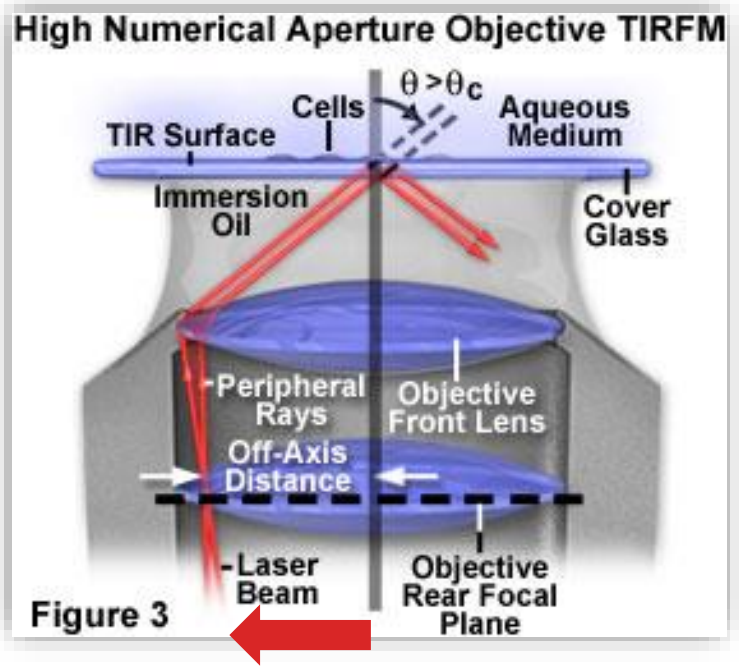

TIRF WIDEFIELD
EPI

INCIDENCE ANGLE OF THE BEAM:

$$r = nf\sin\alpha$$

r: radial distance
n: refractive index of the glass
f: focal lenght og the objective

http://www.microscopyu.com/articles/fluorescence/tirf/tirfintro.html
http://www.olympusmicro.com/primer/techniques/confocal/applications/tirfmintro.html

NUMERICAL APERTURE OF THE OBJECTIVE

glass : water interface

$n_{water\ (2)} = 1.333$

$n_{glass(1)} = 1.515$

$n_{immersion(1)} = 1.515$

$n_{critical} = 61.62^o$

$\boldsymbol{NA(minimum)} = 1.515 * sin61.62^o = \mathbf{1.33}$

$\boldsymbol{NA \sim 1.4}$

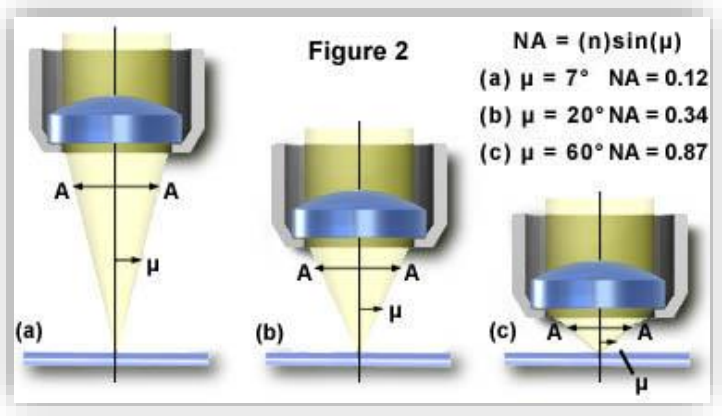

$\boldsymbol{NA \uparrow \rightarrow WD \downarrow}$

glass : cell interface

$n_{cell(2)} = 1.38$

$n_{glass(1)} = 1.515$

$n_{immersion(1)} = 1.515$

$n_{critical} = 65.63^o$

$\boldsymbol{NA(minimum)} = 1.515 * sin65.63^o = \mathbf{1.38}$

$\boldsymbol{NA > 1.4}$!

micro.magnet.fsu.edu/primer/anatomy/numaperture.html

OBJECTIVE-BASED (PRISMLESS) TIRFM

	WD (mm)	NA	n_1 immersion	n_2 cell	critical angle (°)	maximum angle (°)	utilized NA fraction
plan apochromatic	-	1.4	1.515	1.38	65.63	67.53	0.02
UAPON 150xTIRF	0.08	1.45	1.515	1.38	65.63	73.15	0.07
APON 60XTIRF UAPON 100xTIRF	0.1 0.1	1.49	1.515	1.38	65.63	79.57	0.11
APON 100XTIRF	0.08	1.65*	1.788	1.38	50.51	67.34	0.27

* special immersion oil and glass coverslip are needed

The excitation light has to pass through the portion of the numerical aperture cone that is greater than 1.38.

Being on the edge gives less flexibility.

REMINDER: NEXT SLIDE

AVAILABLE NUMERICAL APERTURE MARGIN

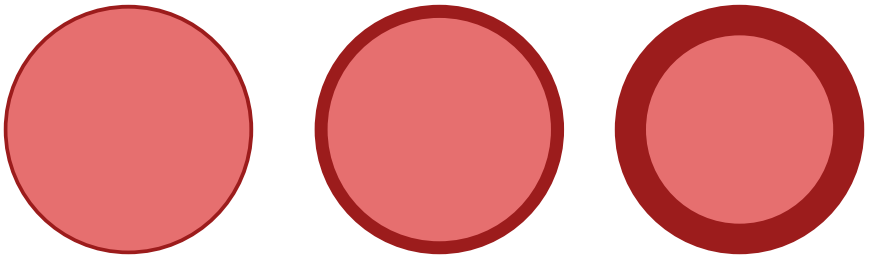

NA = 1.4 **NA = 1.45** **NA = 1.65**

INFLUENCES ON THE THE „EVANESCENT" NATURE

$$d = \frac{\lambda}{4\pi n_1}\left(\sin^2\alpha_1 - \left(\frac{n_2}{n_1}\right)^2\right)^{-\frac{1}{2}}$$

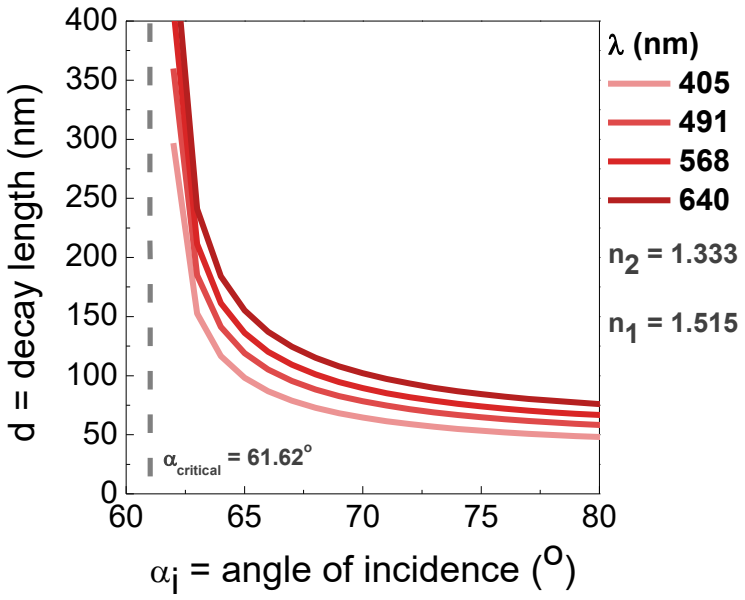

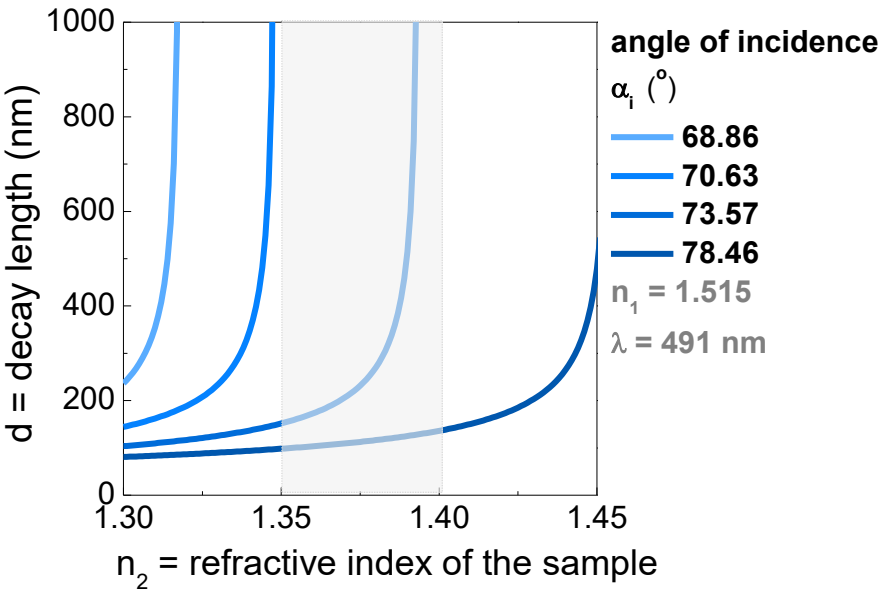

As the angle of incidence increases, the depth becomes narrower (resolution!)

$$\boldsymbol{\alpha_1 \rightarrow \alpha_{critical}}\text{: } \boldsymbol{d \rightarrow \infty}$$

As the wavelength increases, the depth is narrower (resolution!)

As n_2 increases, the depth increases (resolution!).

As the angle of incidence increases, the sensitivity of the evanescent field to n_2 decreases.

PRISM vs. OBJECTIVE-BASED TIRFM

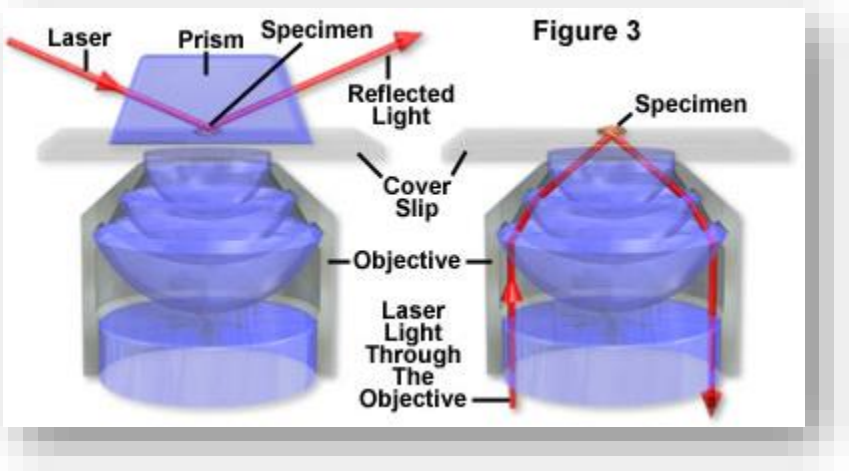

	PRISM-BASED TIRFM	OBJECTIVE-BASED TIRF
SYSTEM SETUP, ALIGMENT, MAINTENANCE	-	+
ANGLE OF INCIDENCE	+	-
ACCESS TO THE SAMPLE	-/+	+
LASER SAFETY	-	+
OBJECTIVE NEEDS	high working distance	high NA

http://www.microscopyu.com/articles/fluorescence/tirf/tirfintro.html
http://www.olympusmicro.com/primer/techniques/confocal/applications/tirfmintro.html

SAMPLE PREPARATION

ENVIRONMENT
- immersion
- incubator
- autofocus

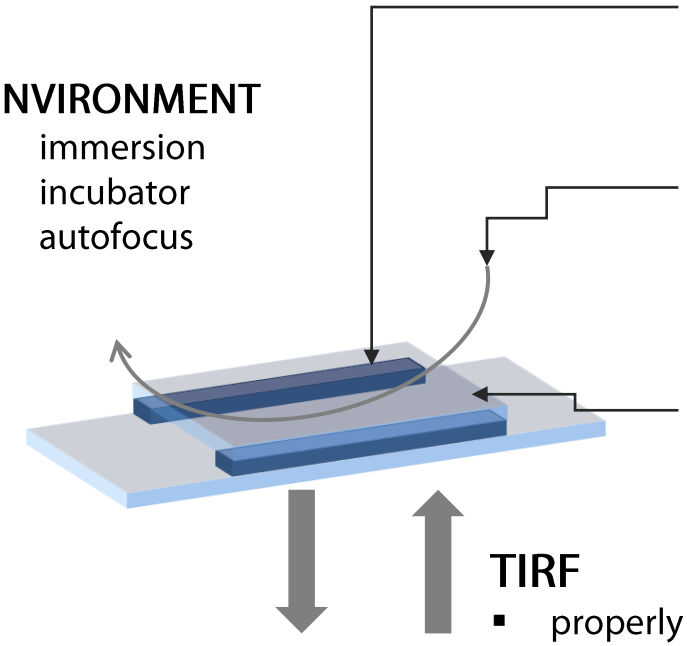

SAMPLE (cells, proteins, …)
- fluorescently labeled, no restriction of usable fluorphores (!available wavelength, and filter set)
- oxigen scavenger system
- low refractive index medium

FLOW CELL
- manual / microfluidics

SURFACE CHEMISTRY
- poly-L-lysine (PLL)
- collagen/fibronectin
- PLL-g-PEG
- streptavidine-biotin
- NEM-myosin

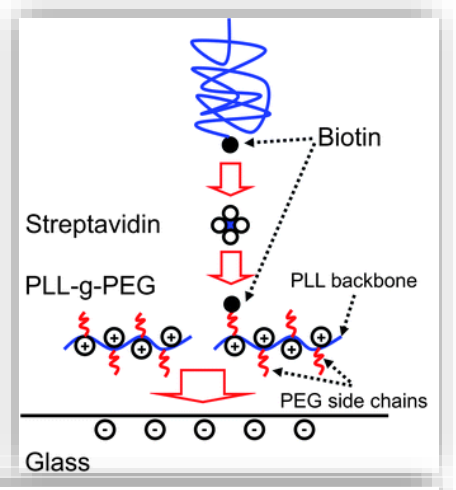

TIRF
- properly aligned laser beam
- no optical imperfections
- properly mounted coverslip (no tilt!)

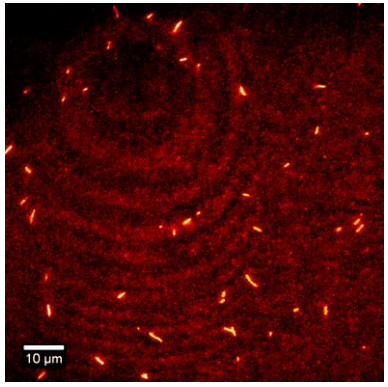

- interference fringes
- inhomogeneous field

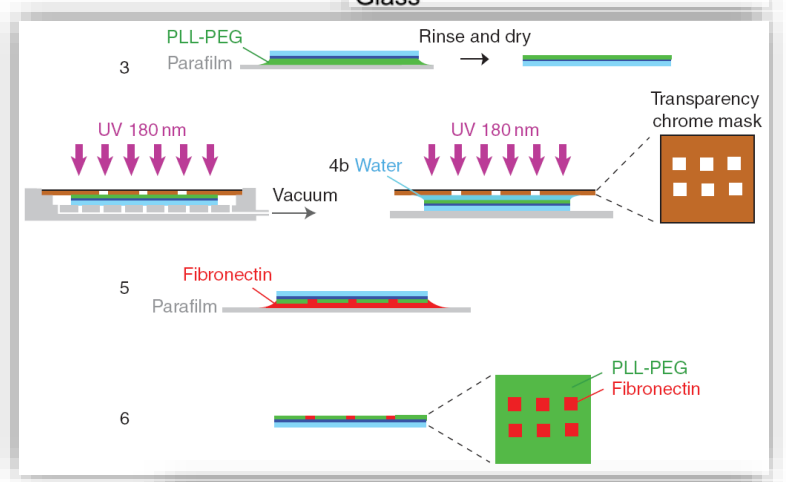

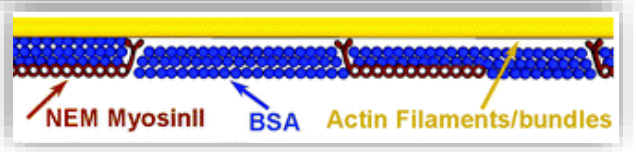

Azioune et al. Lab on a Chip 2009
Reymann AC. et al. Nature Materials 2010

TIRFM – PROTEIN BIOCHEMISTRY

TIRFM IN STUDYING CYTOSKELETAL POLYMER DYNAMICS

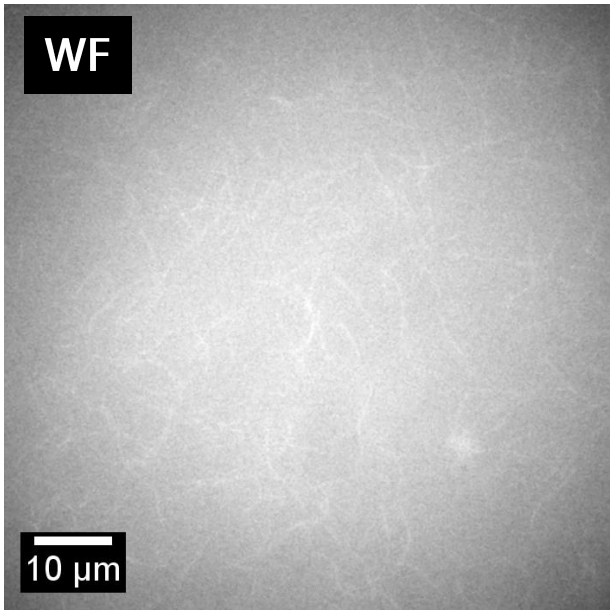

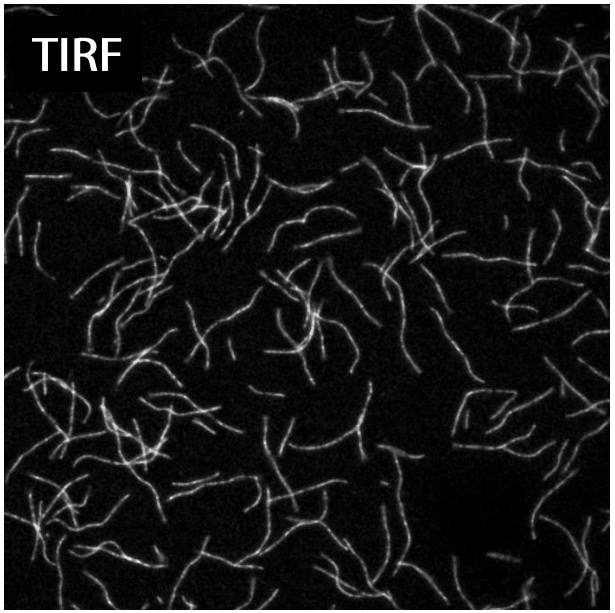

CYTOSKELETAL POLYMERS

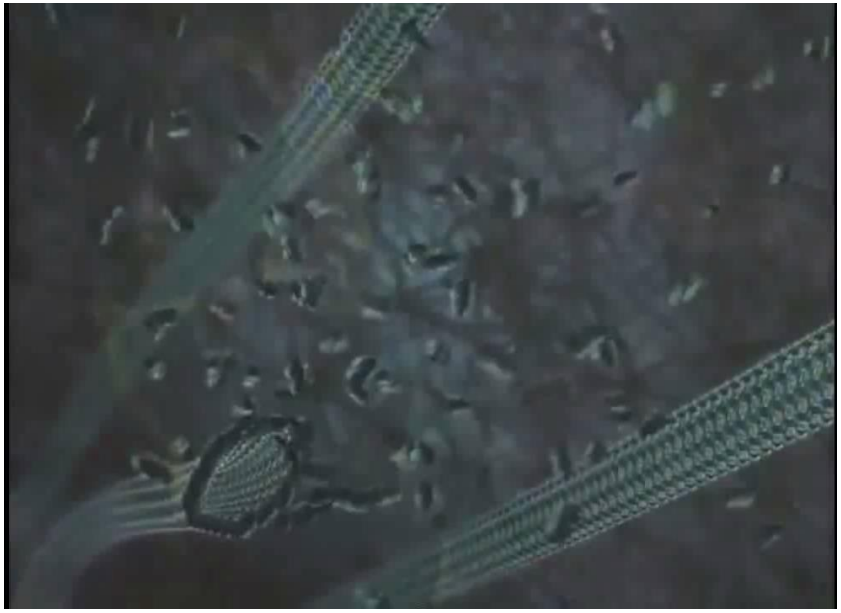

ACTIN BIOCHEMISTRY

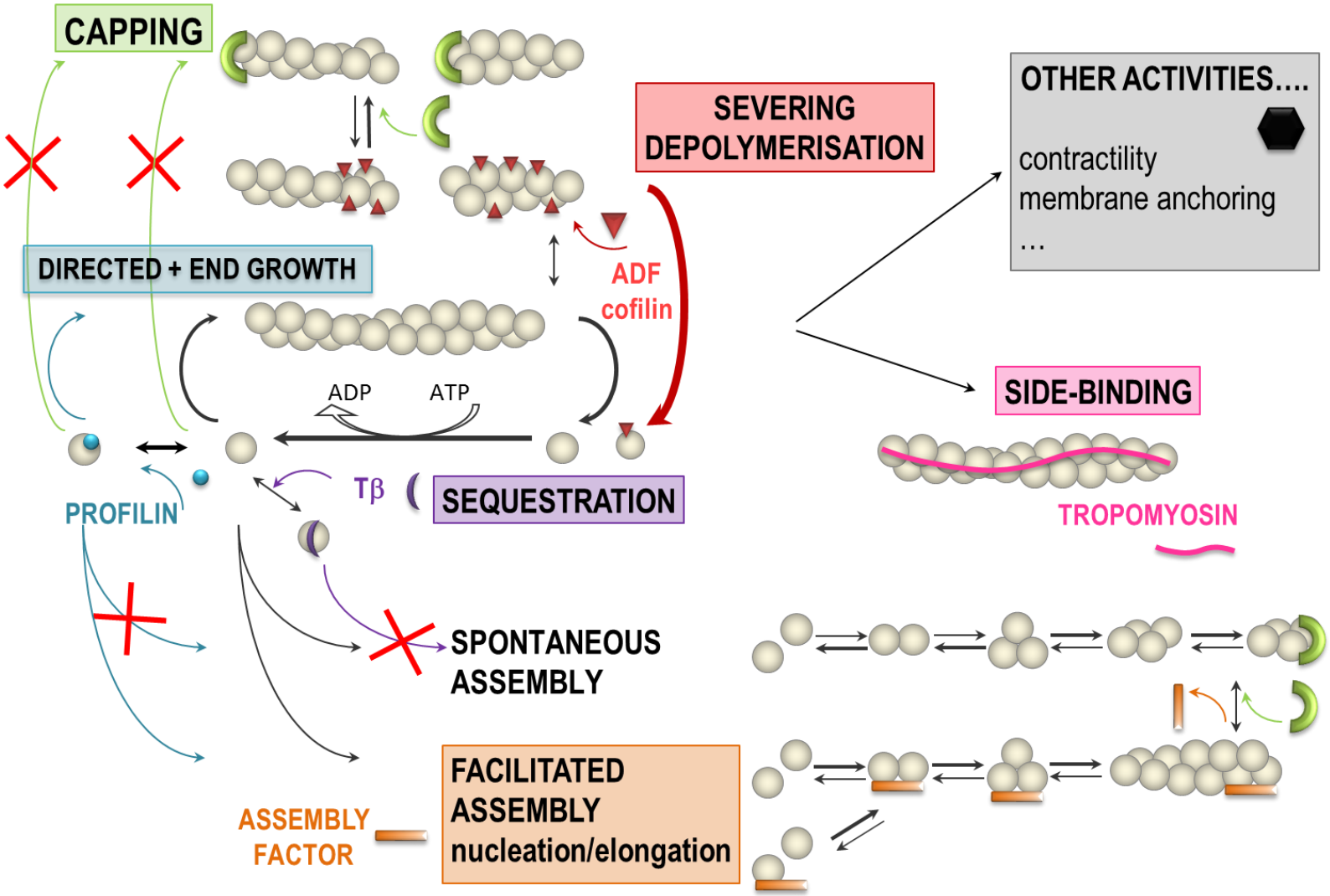

Renault L. Bugyi B. Carlier MF. *Trends in CB* 2008

ACTIN BIOCHEMISTRY

SPONTANEOUS ACTIN ASSEMBLY

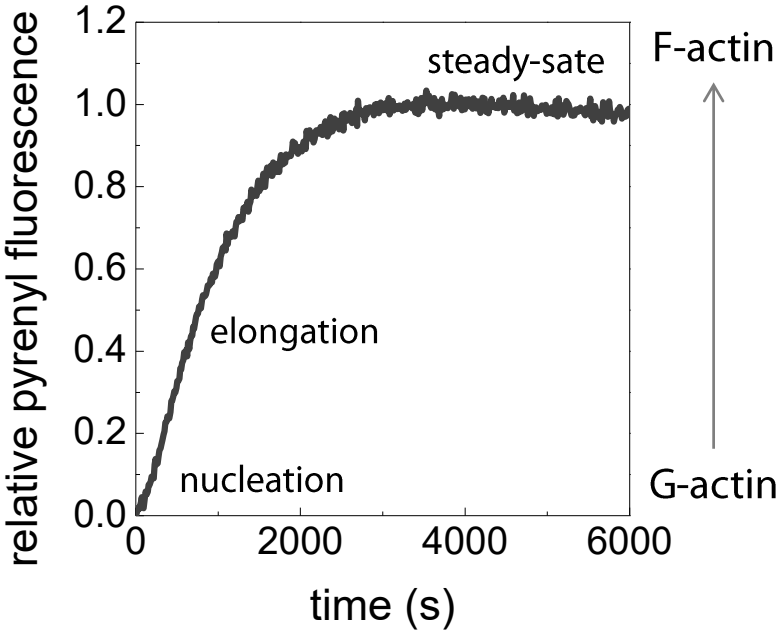

$$v = k_+[G_0 - c_c][F] - k_-[F]$$

ACTIN BIOCHEMISTRY

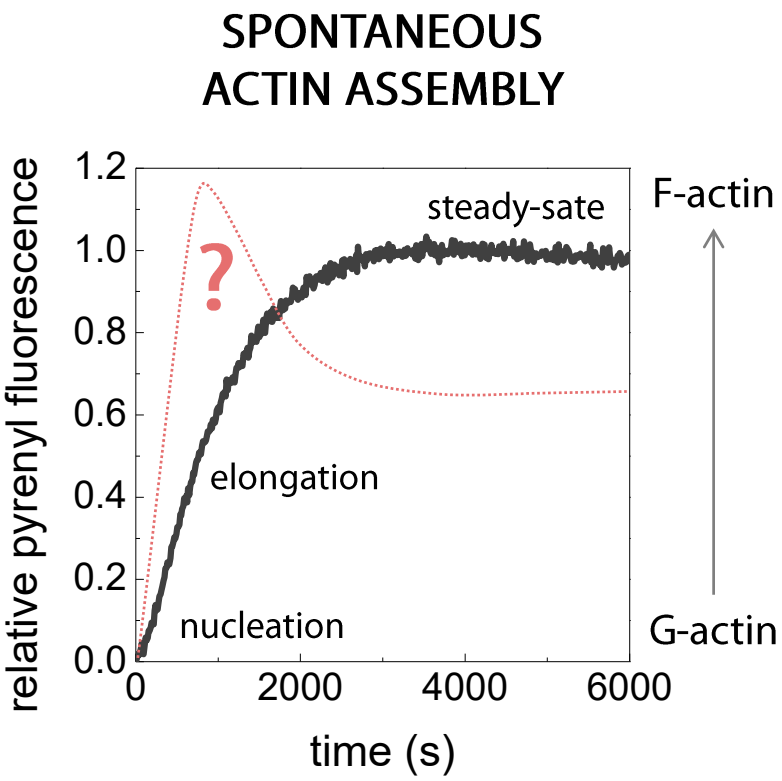

$$v = k_+[G_0 - c_c][F] - k_-[F]$$

ACTIN BIOCHEMISTRY

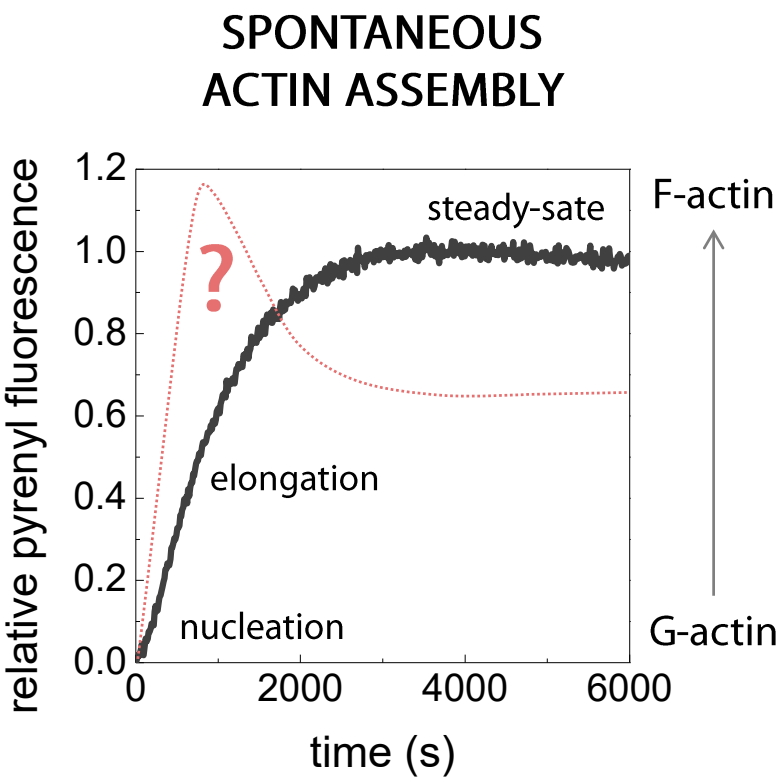

$$v = k_+[G_0 - c_c][F] - k_-[F]$$

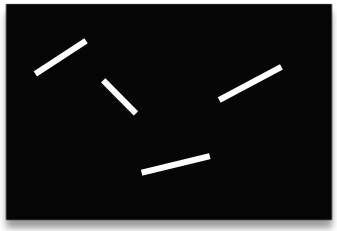

SPONTANEOUS ACTIN ASSEMBLY

k_+, k_-, [F], [G_0], [c_c]

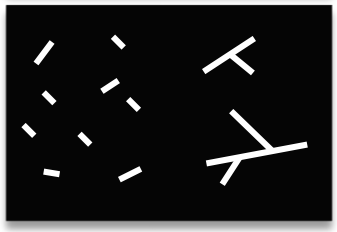

NUCLEATION FACTORS

[G_0], [F]

formins, Arp2/3

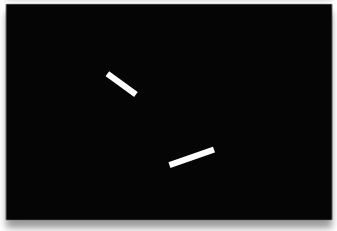

SEQUESTRATORS

[G_0], [F]

WH2 domain proteins

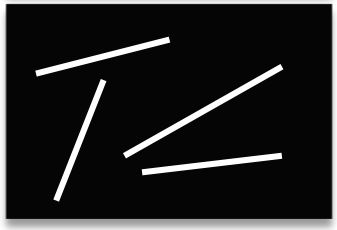

ELONGATION FACTORS

k_+, k_-, [F]

formins, VASP, CP

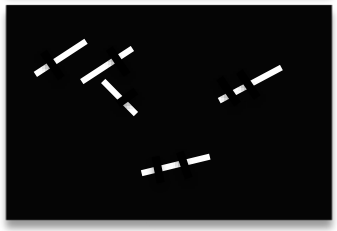

FILAMENT BINDING

k_-, [F], [c_{ss}]

depolymerisation, severing, binding

ACTIN BIOCHEMISTRY

SPONTANEOUS GROWTH OF ACTIN FILAMENTS

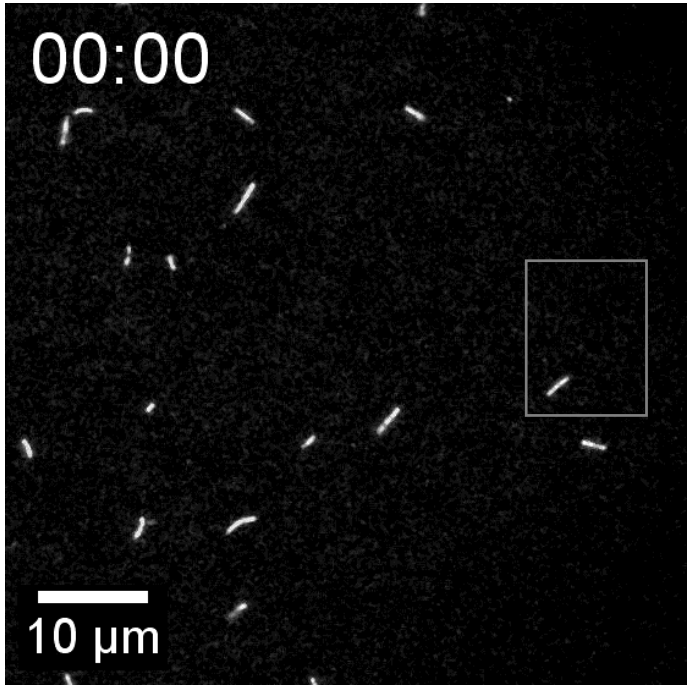

time = min : s
AlexaNHS488-ACTIN (10 % LABELED)
491 nm 60xNA1.45
t = 100 ms, I = 10% (P = 15 mW)
HamamatsuCCD

- POLYMER GROWTH, SHRINKAGE RATE

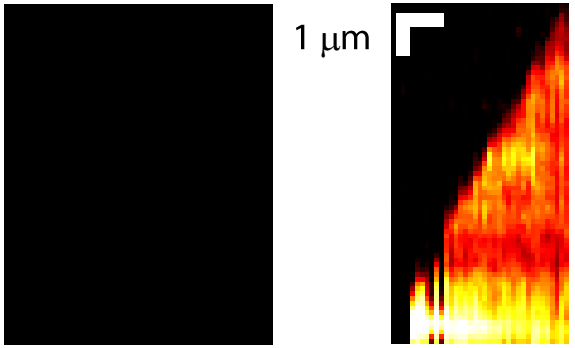

- POLYMER NUMBER

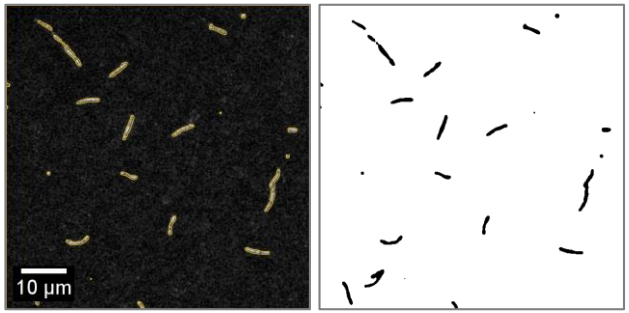

- POLYMER STRUCTURAL FEATURES

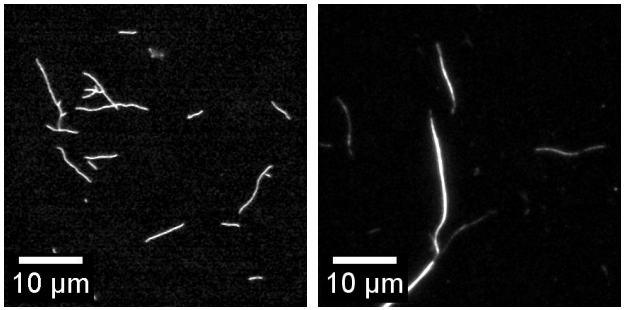

NEURONAL CYTOSKELETON

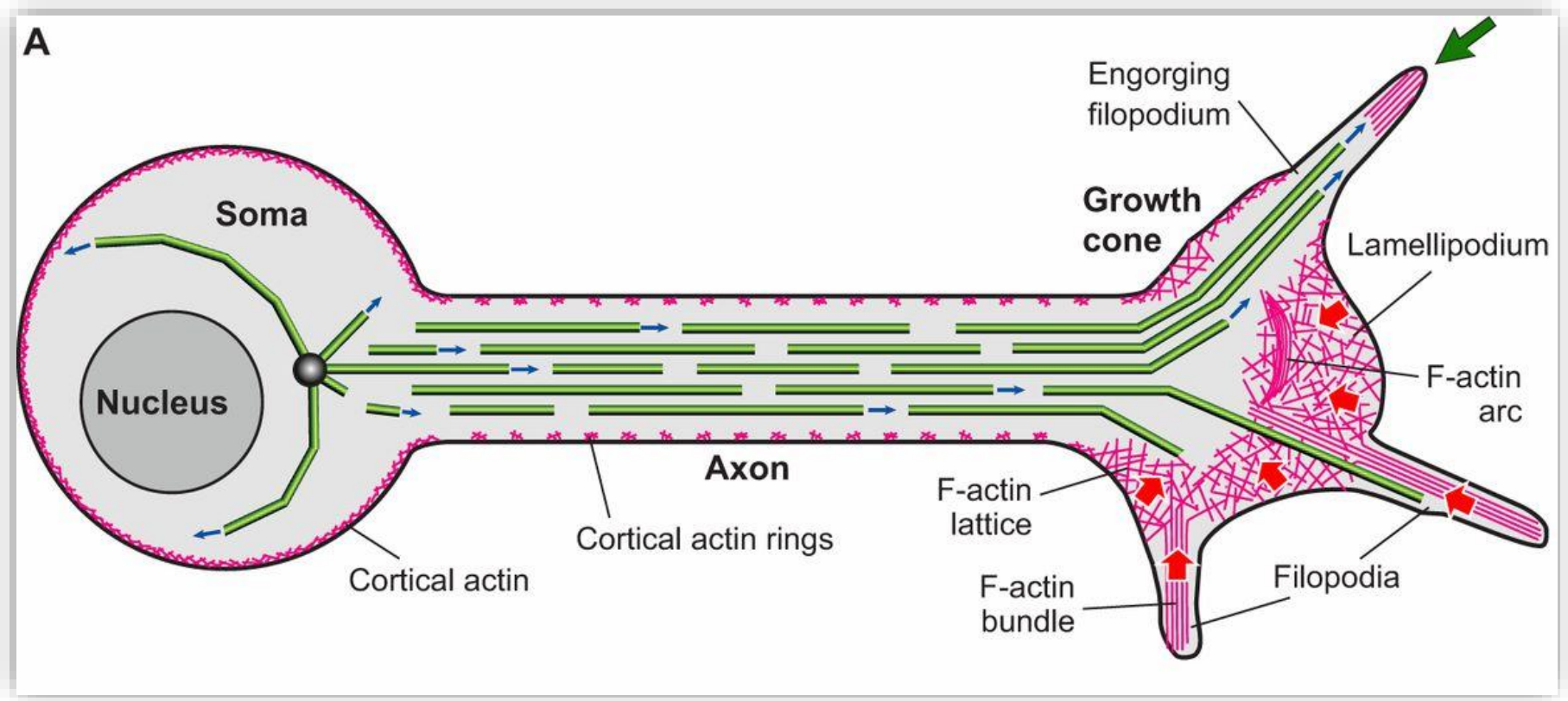

Prokop A. et al. Journal of Cell Science 2013

NEURONAL CYTOSKELETON - DAAM formin in axonal filopodia formation

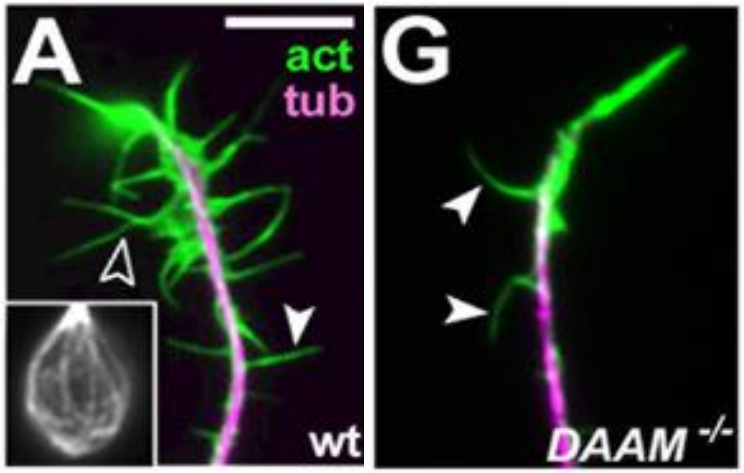

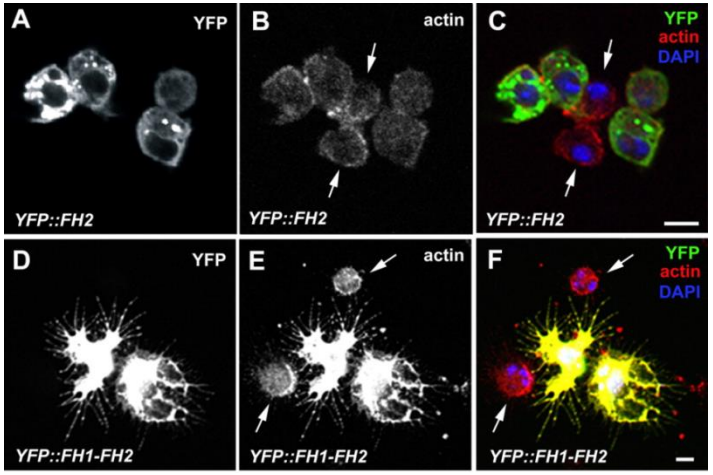

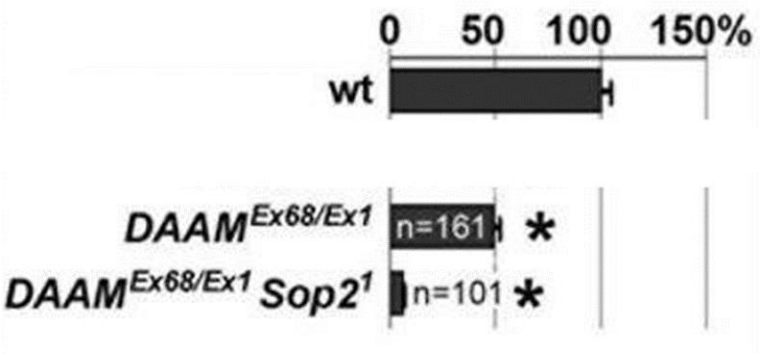

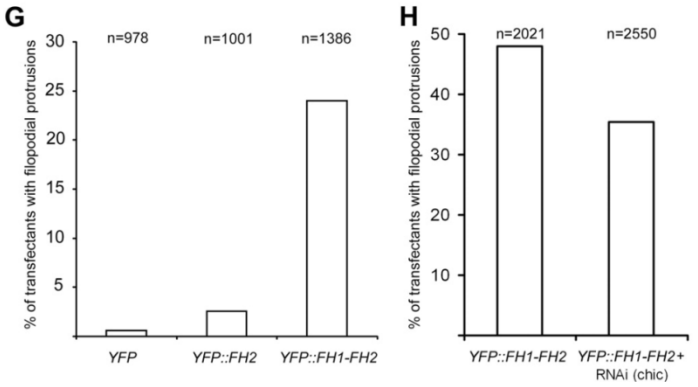

Barkó Sz. Bugyi B. et al. Journal of Biological Chemistry 2010
Goncalves-Pimentel et al. PLOS One 2011

DAAM enhances actin nucleation, but inhibits filament elongation

AlexaNHS488-ACTIN (10 % LABELED)

ACTIN

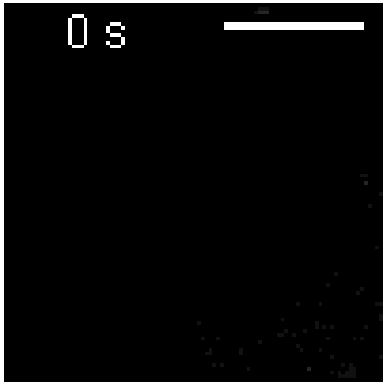

1.2 μM actin

v = 12.68 ± 0.96 su/s

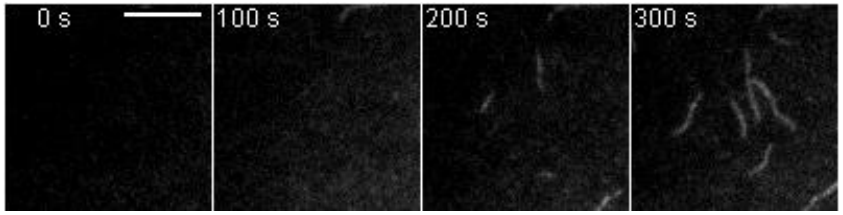

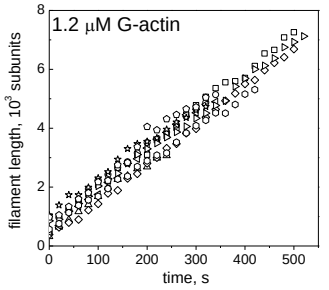

DAAM FH2

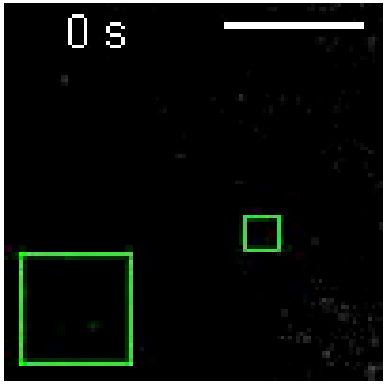

1.2 μM actin + 2.34 μM DAAM FH2

v = 0.59 ± 0.22 su/s

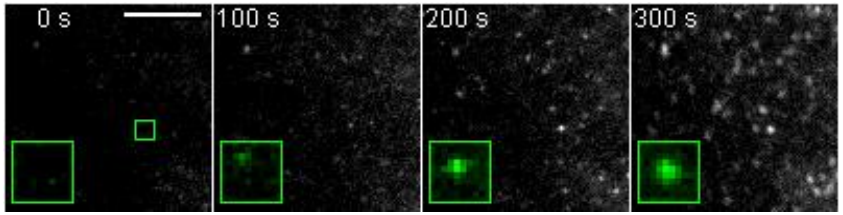

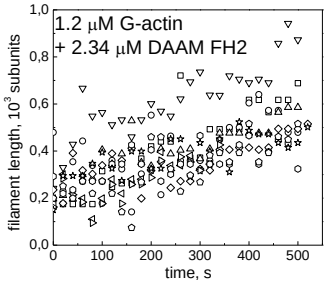

DAAM FH1-FH2

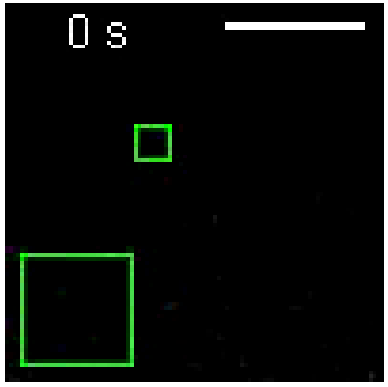

1.2 μM actin + 2.4 μM DAAM FH1-FH2

v = 0.99 ± 0.32 su/s

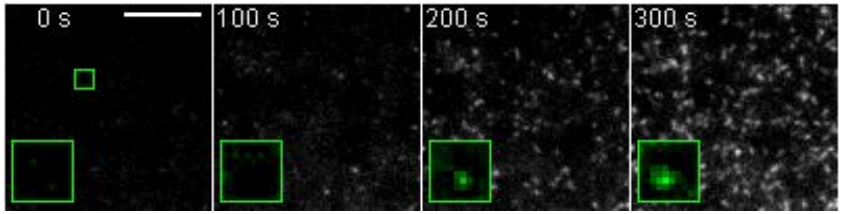

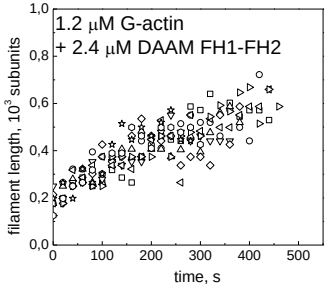

Barkó Sz. Bugyi B. et al. Journal of Biological Chemistry 2010

Formins processively associate to actin filament plus ends

AlexaNHS488-ACTIN (10 % LABELED)
FORMIN

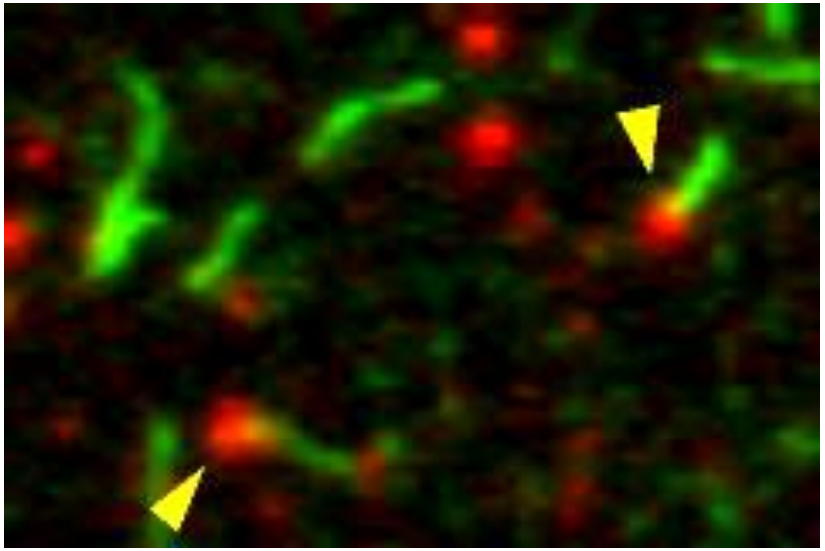

Profilin acts as a molecular switch in the activity of DAAM FH1-FH2

ACTIN

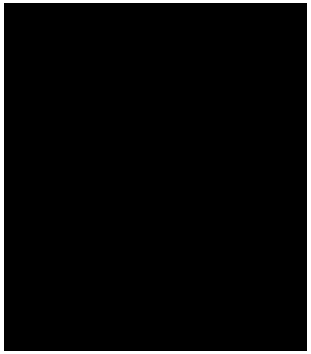

0.3 μM actin + 0.72 μM profilin

AlexaNHS488-ACTIN (10 % LABELED)
AlexaNHS568-ACTIN (10 % LABELED)

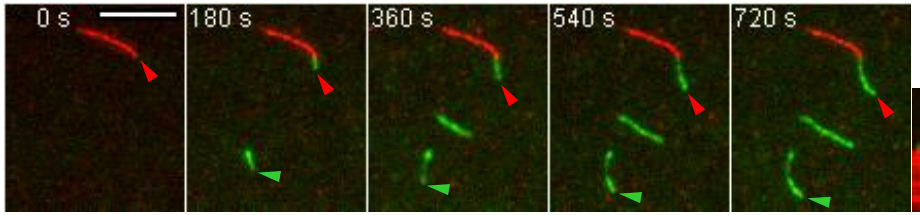

v = 2.91 ± 0.50 su/s

10 μm
500 s

DAAM
FH2

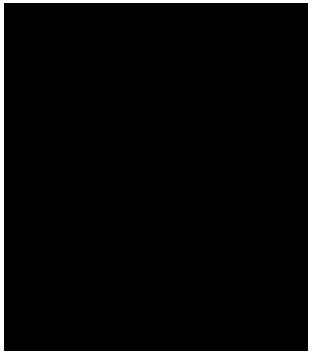

0.3 μM actin + 0.72 μM profilin + 2.6 μM DAAM FH2

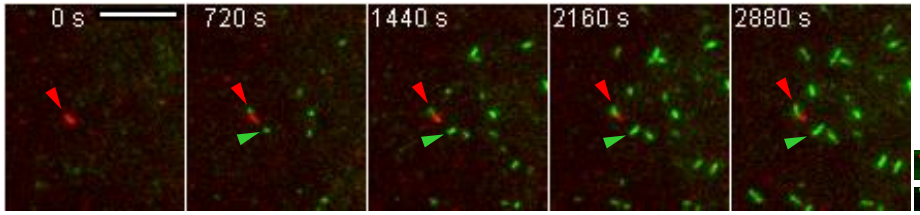

v = 0.20 ± 0.05 su/s

DAAM
FH1-FH2

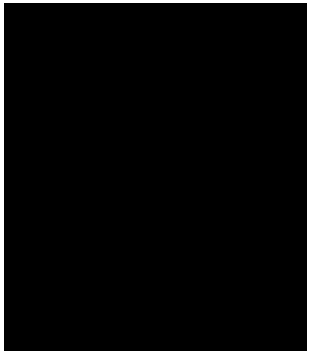

0.3 μM actin + 0.72 μM profilin + 2.4 μM DAAM FH1-FH2

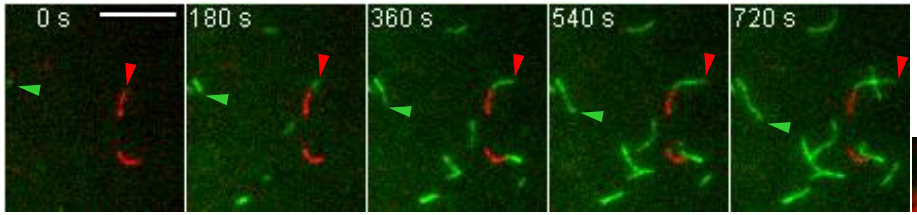

v = 2.35 ± 0.28 su/s

Barkó Sz. Bugyi B. et al. Journal of Biological Chemistry 2010

The C-terminal of DAAM further tunes the activity of the FH1-FH2 region

ACTIN

DAAM
FH1-FH2

DAAM
FH1-FH2-DAD-CT

DAAM
DAD-CT

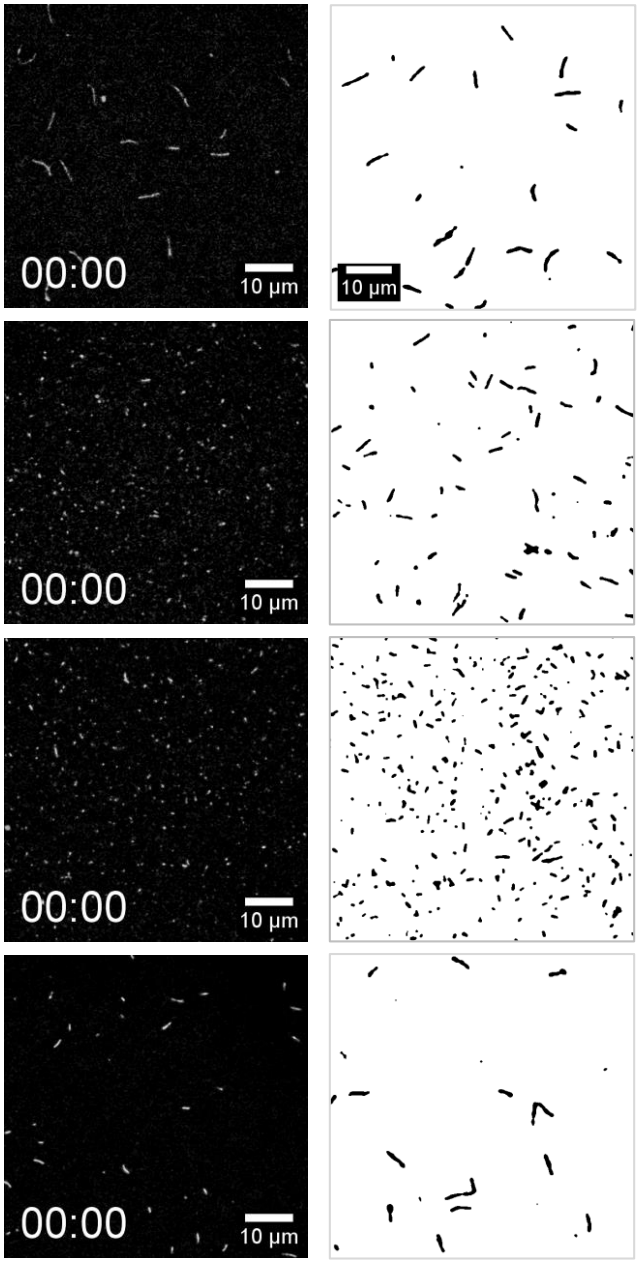

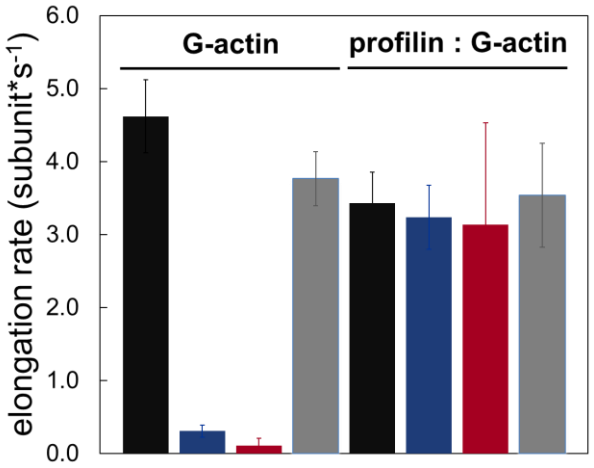

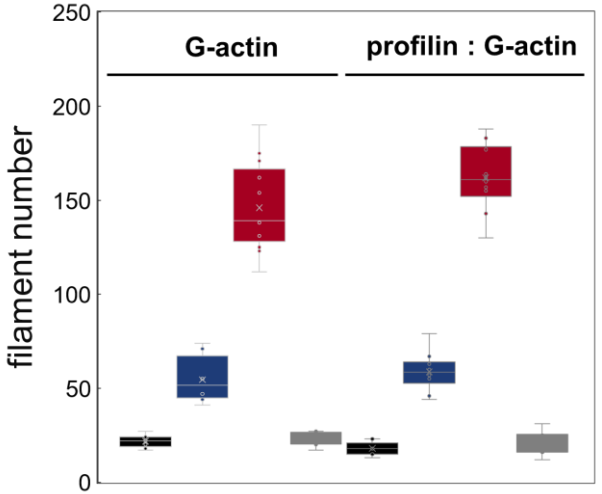

Vig A. Bugyi B. et al. manuscript in preparation 2016

The C-terminal of DAAM essential for mediating actin-microtubule crosstalk

AlexaNHS488-ACTIN (10 % LABELED)
AlexaNHS568-MICROTUBULE (10 % LABELED)

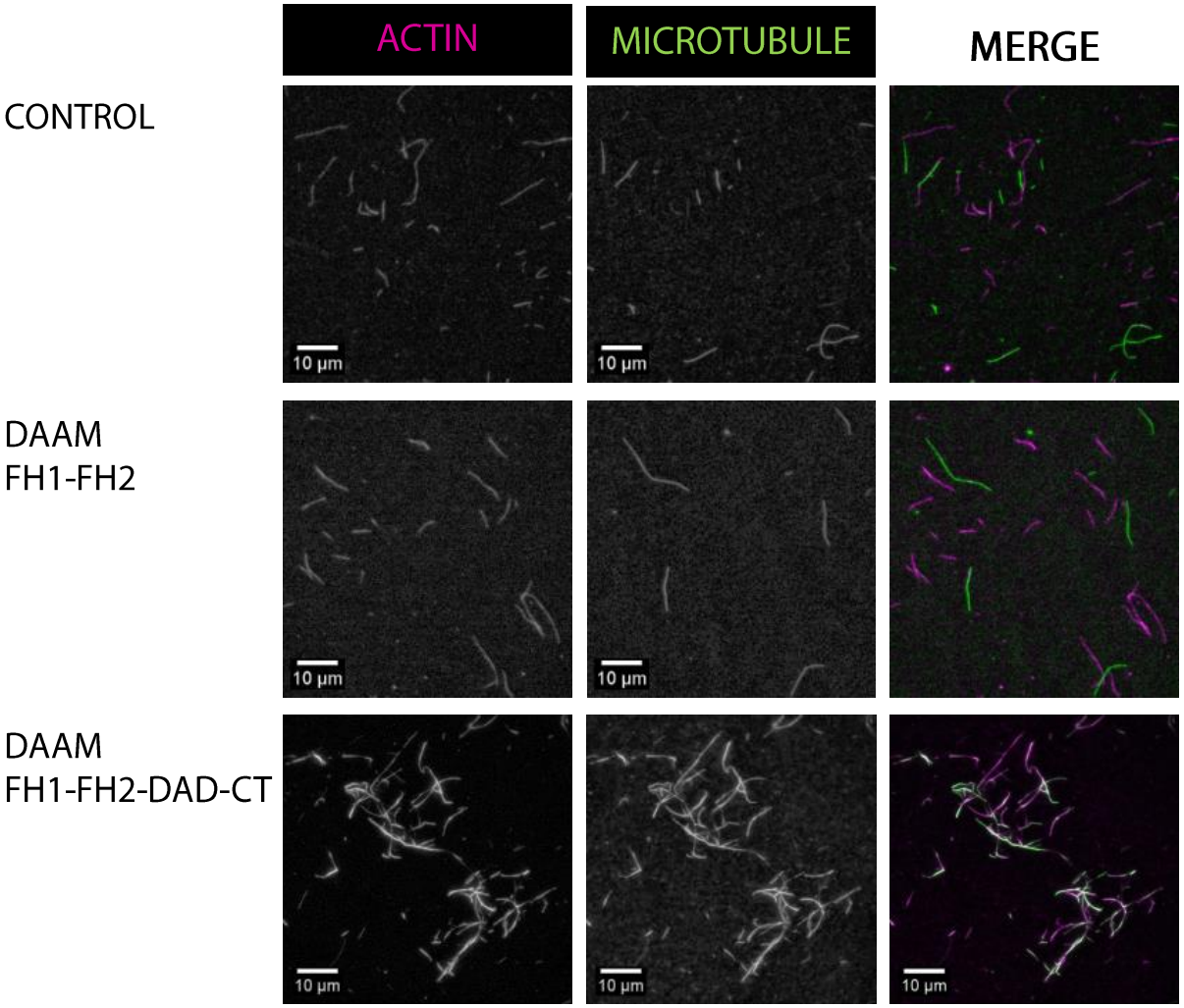

Vig A. Bugyi B. unpublished

The model of DAAM mediated axonal filopodia formation

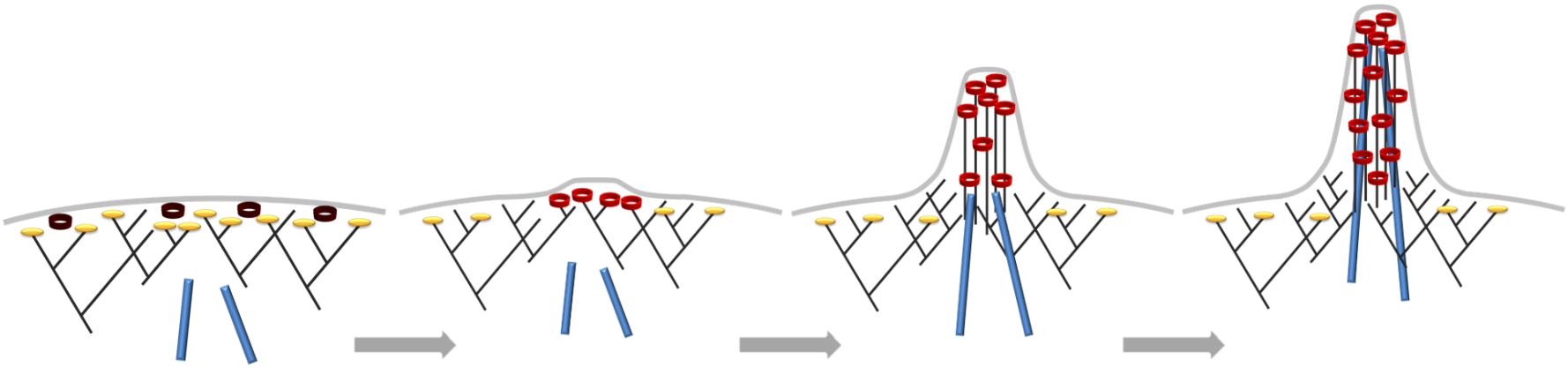

Vig A. Bugyi B. unpublished

TIRFM - MICROPATTERNING

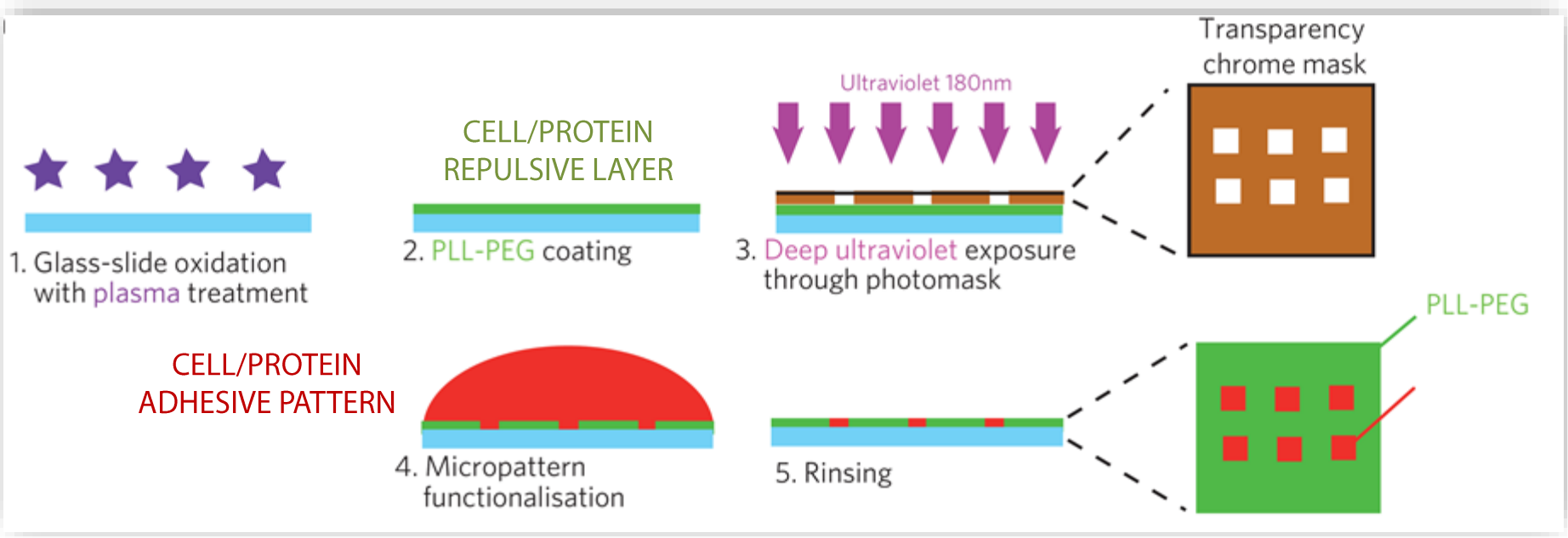

Azioune et al. Lab on a Chip 2009
Reymann AC. et al. Nature Materials 2010

Nucleation geometry governs ordered actin networks structures

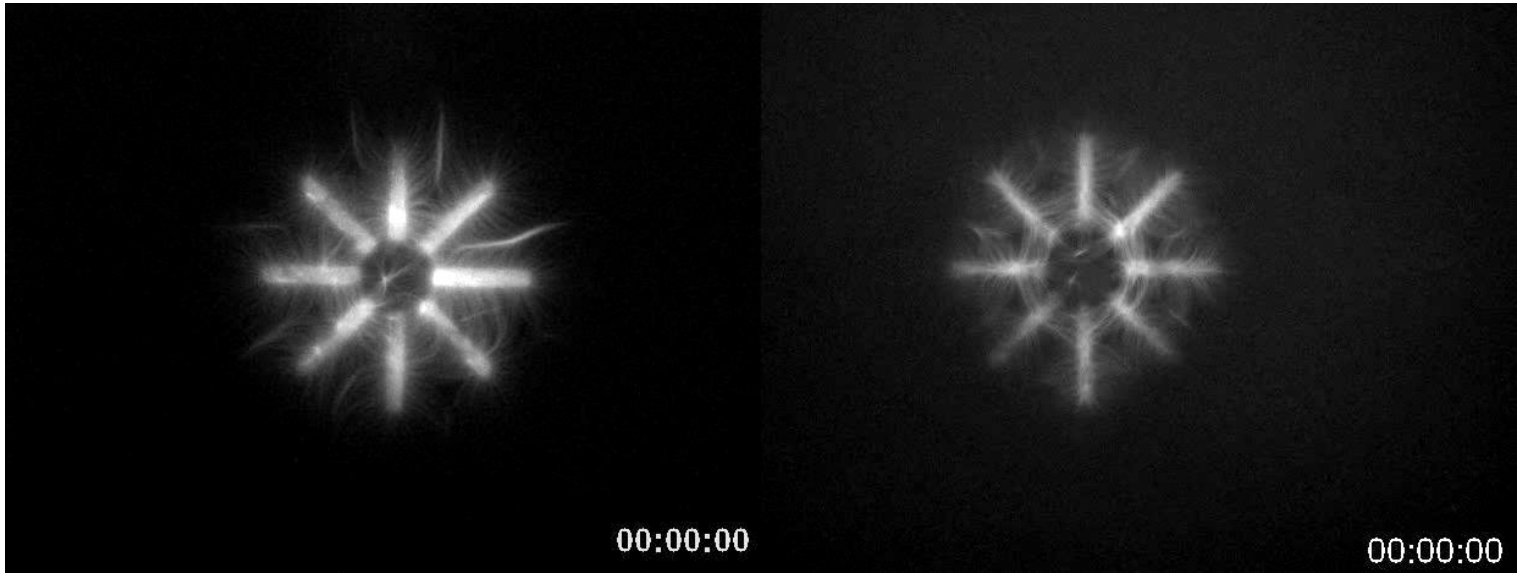

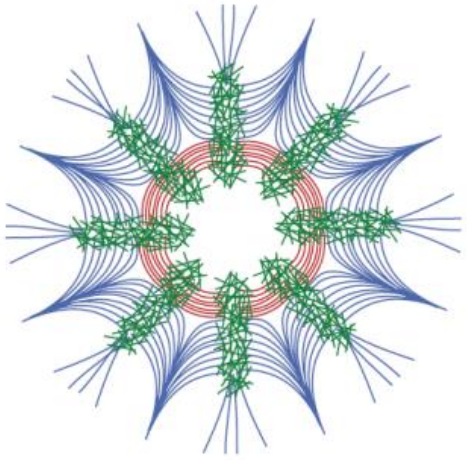

ANGLE (direction!)
BETWEEN FILAMENTS

Actin filaments :

anti-parallel

parallel

branched
meshwork

PARALLEL

BRANCHED

ANTIPARALLEL

Reyman AC Science 2012
Reymann AC. et al. Nature Materials 2010

Actin network architecture can determine myosin motor activity

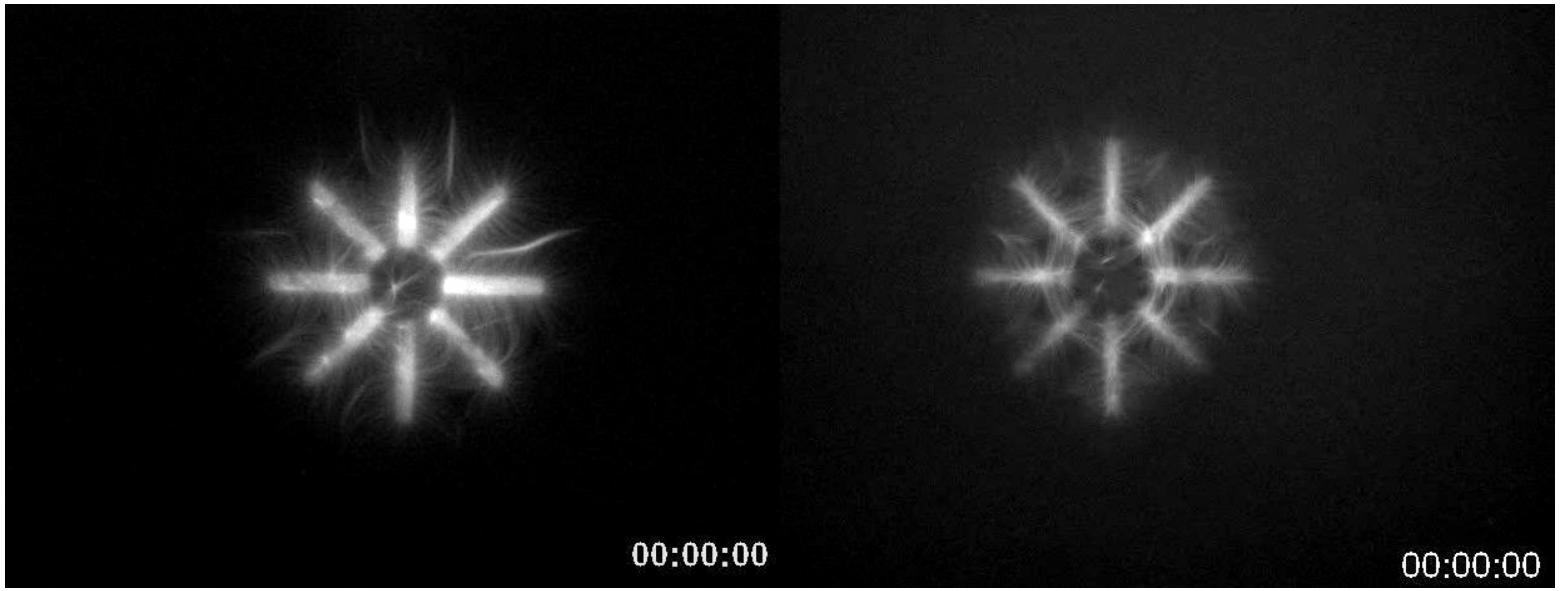

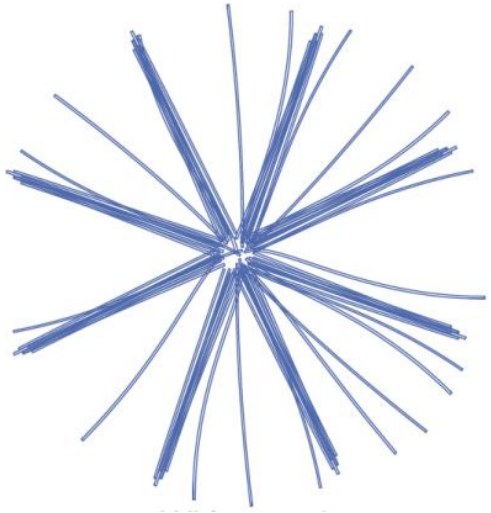

ANGLE (direction!)
BETWEEN FILAMENTS

Actin filaments :

anti-parallel

parallel

branched
meshwork

PARALLEL

BRANCHED

ANTIPARALLEL

Reyman AC Science 2012
Reymann AC. et al. Nature Materials 2010

Reconstitution of the actomyosin-dependent formation of the mechanosensitive talin–vinculin complex

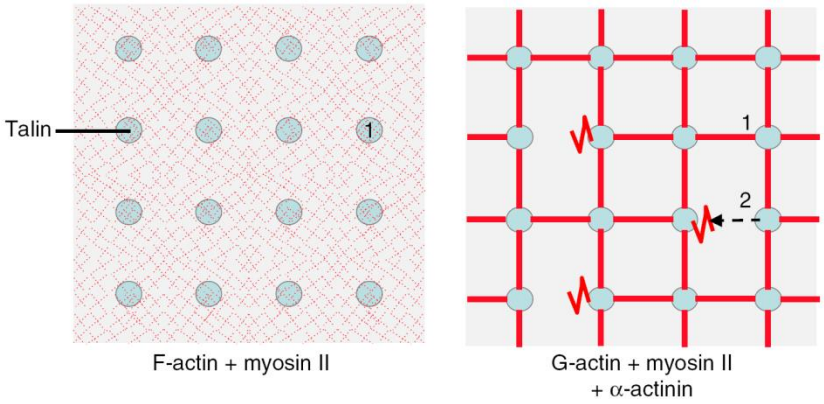

IN VITRO RECONSTITUTION OF THE ACTOMYOSIN-DEPENDENT BINDING OF VINCULIN TO TALIN.

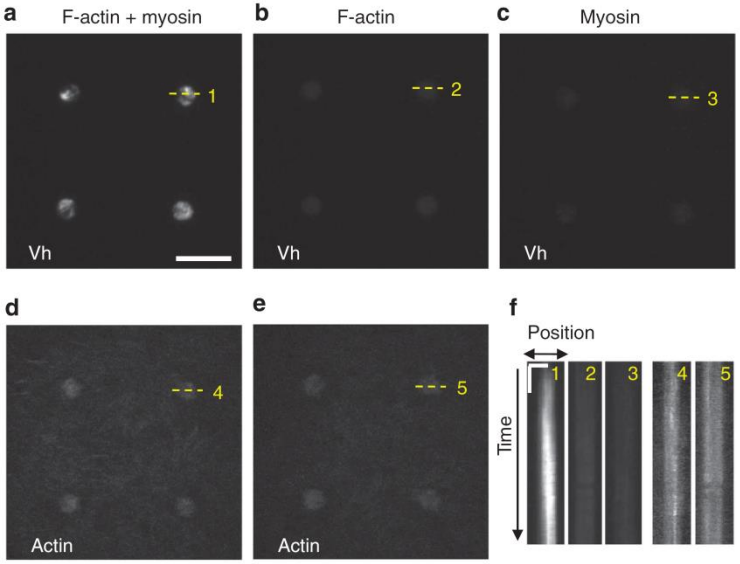

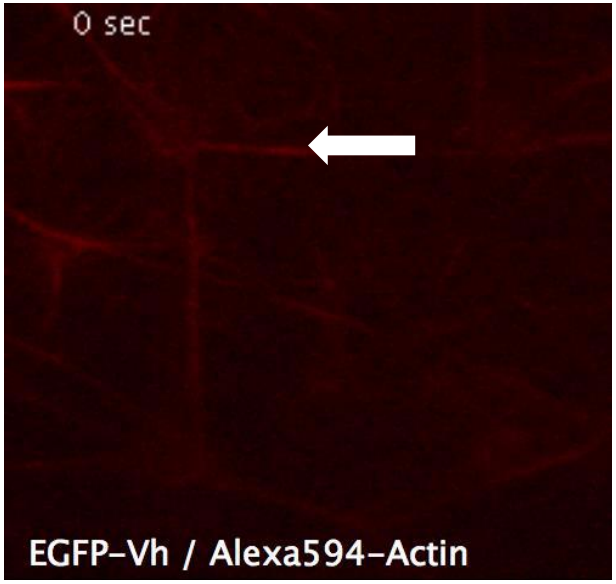

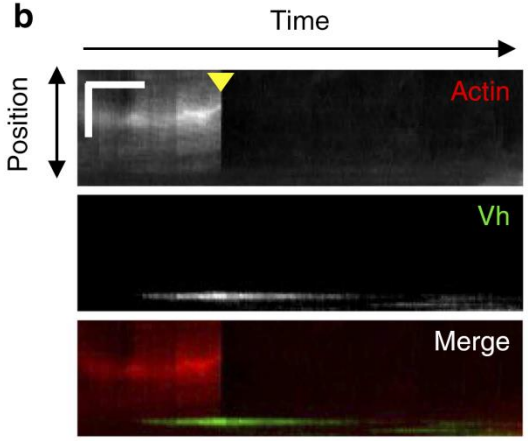

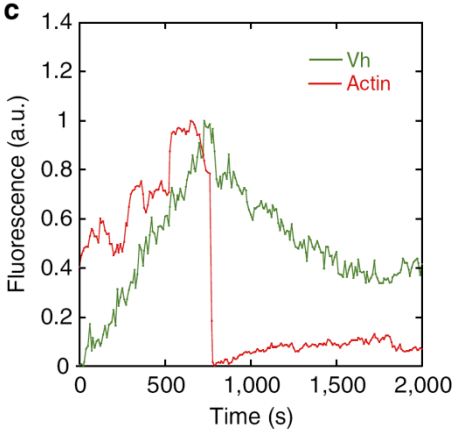

Le Clainche C. Nature Communication 2014

Reconstitution of the actomyosin-dependent formation of the mechanosensitive talin–vinculin complex

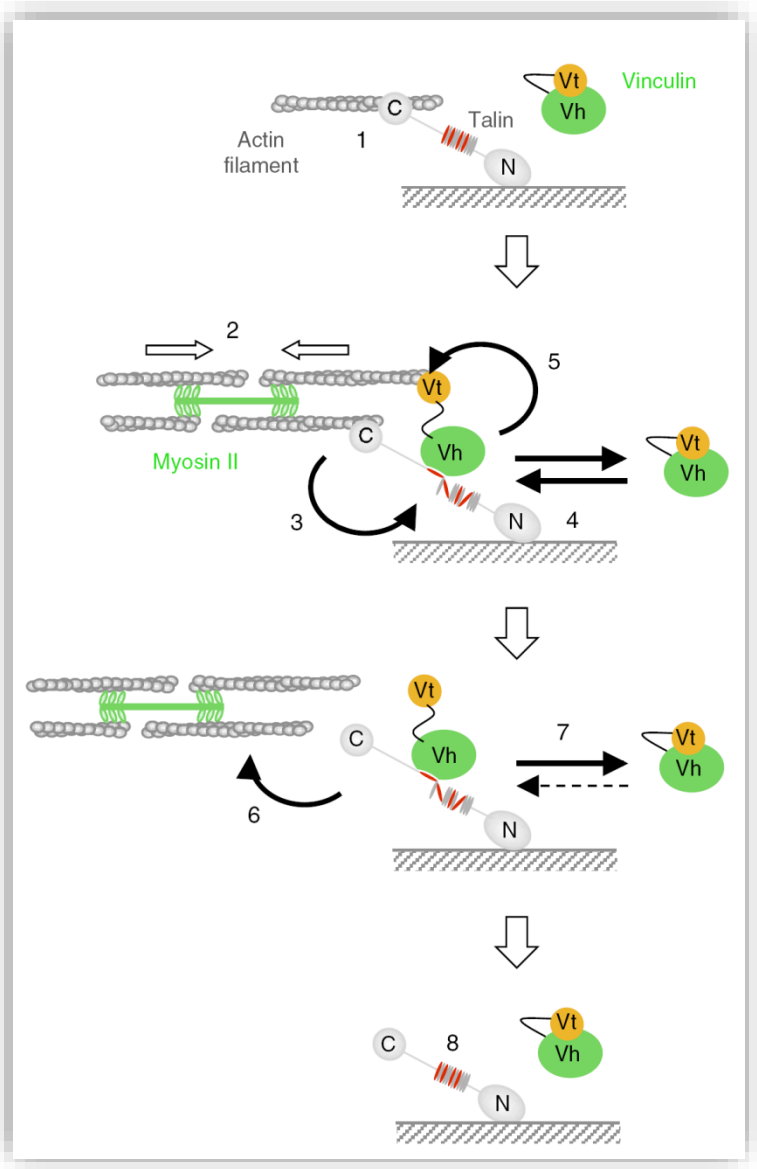

Le Clainche C. Nature Communication 2014

Nanometer targeting of microtubules to focal adhesions

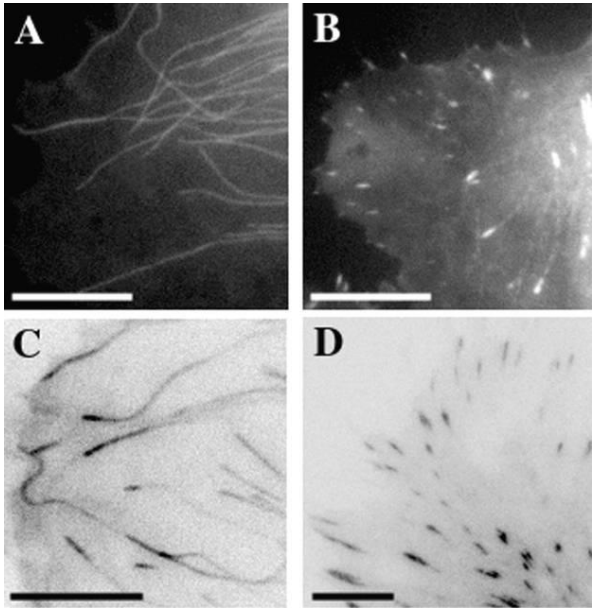

TIRFM reveals microtubule tips and focal adhesions within 150 nm of the dorsal cell surface. Fibroblasts were transfected with either GFP-tubulin (A and C) or GFP-zyxin (B and D). Live-cell images were taken either with standard wide field epi-illumination (A and B) or TIRFM (C and D). For clarity, TIRFM images are shown in reverse contrast. Bar, 10 µm.

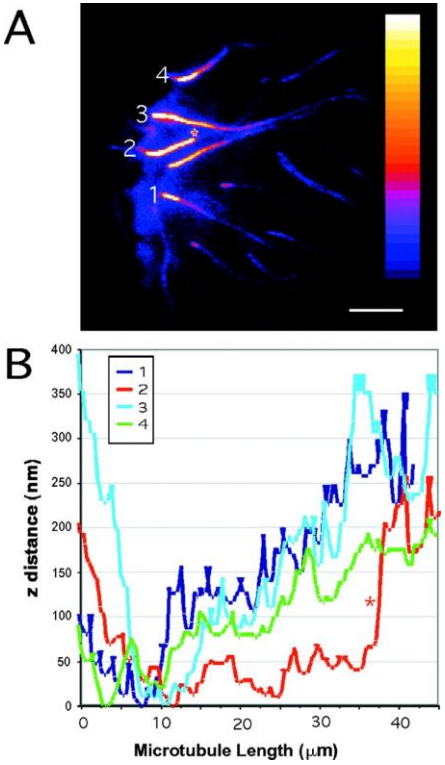

model IX2; Olympus
100x NA 1.65
high refractive index immersion oil (diodomethane; Sigma-Aldrich)
special high NA coverslips (*n* = 1.788; Olympus)
multi-line laser (Innova 70C; Coherent)
CCD camera (MicroMAX 1024B; Princeton Instruments).

Krylyshkina et al. **Nanometer targeting of microtubules to focal adhesions.** JCB 2003

Filopodia contribute to the construction of contractile bundles in the lamella

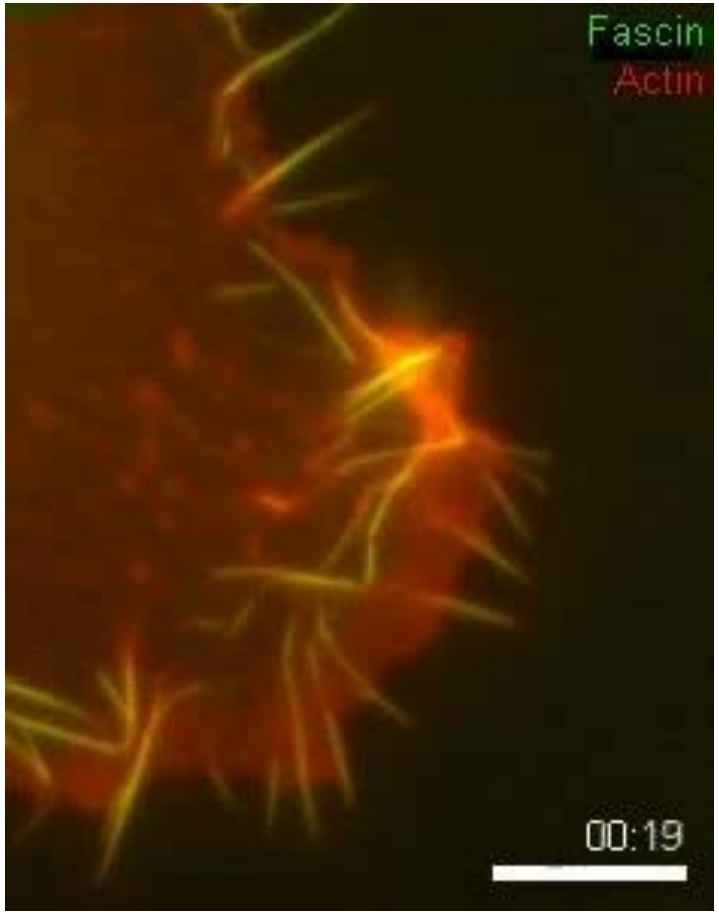

TRANSITION OF FILOPODIA INTO THE LAMELLA

mCherry-actin GFP-fascin

Arrowheads indicate two bundles that form from filopodia folding in opposite directions into the cell edge. As the cell edge advances, fascin dissociates from the bundles, which subsequently develop into stress fibers in the lamella cytoskeleton. Time-lapse images were acquired every 10 s and the total duration of the video is 32 min. The display rate is 6 frames/s. Bar, 10 µm.

100x 1.46 NA objective 100x (Carl Zeiss, Inc.)
488- and 568-nm laser lines (Laser Physics USA)
rear-illuminated CCD camera (Cascade 512B; Roper Scieintific)
a dual imager for simultaneous imaging the channels (Optical Insights)

Nemethova et al. JCB 2008.

Filopodia contribute to the construction of contractile bundles in the lamella

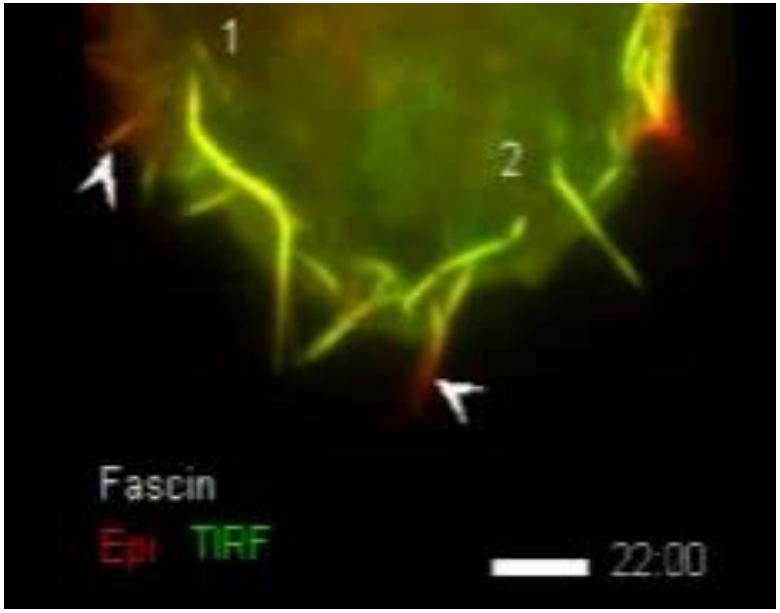

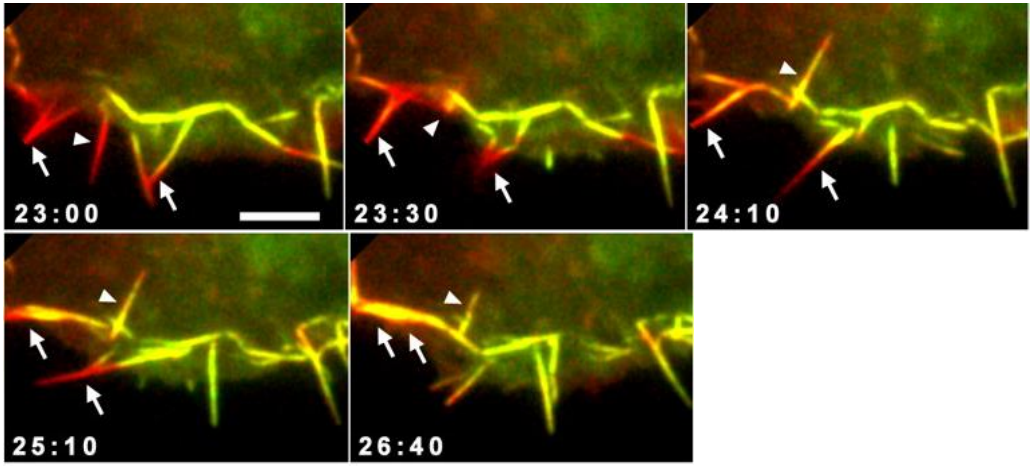

ENTRY OF FILOPODIA INTO VENTRAL LAYER OF THE CYTOSKELETON

Filopodia fold down into the zone of the evanescent wave to within 200 nm from the substrate. Periphery of a fibroblast, transfected with EGFP-fascin and imaged simultaneously by **TIRF and epifluorescence** Arrowheads indicate examples of filopodia folding down into the ventral cytoskeleton at the base of the lamellipodium. Filopodium marked with arrowhead folds upwards and then backward into the cell; filopodia marked with arrows fold laterally and down into the cell edge. Time-lapse images were acquired every 10 s and the total duration of the video was 54 min. The display rate is 6 frames/s. Bar, 5 µm.

100x 1.46 NA objective 100x (Carl Zeiss, Inc.)
488- and 568-nm laser lines (Laser Physics USA)
rear-illuminated CCD camera (Cascade 512B; Roper Scieintific)
a dual imager for simultaneous imaging the channels (Optical Insights)

Nemethova et al. JCB 2008.

TIRFM - SINGLE MOLECULE LOCALIZATION MICROSCOPY

STORM – STOCHASTIC OPTICAL RECONSTRUCTION MICROSCOPY
PALM – PHOTOACTIVATED LOCALIZATION MICROSCOPY

ATP turnover rate of myosin

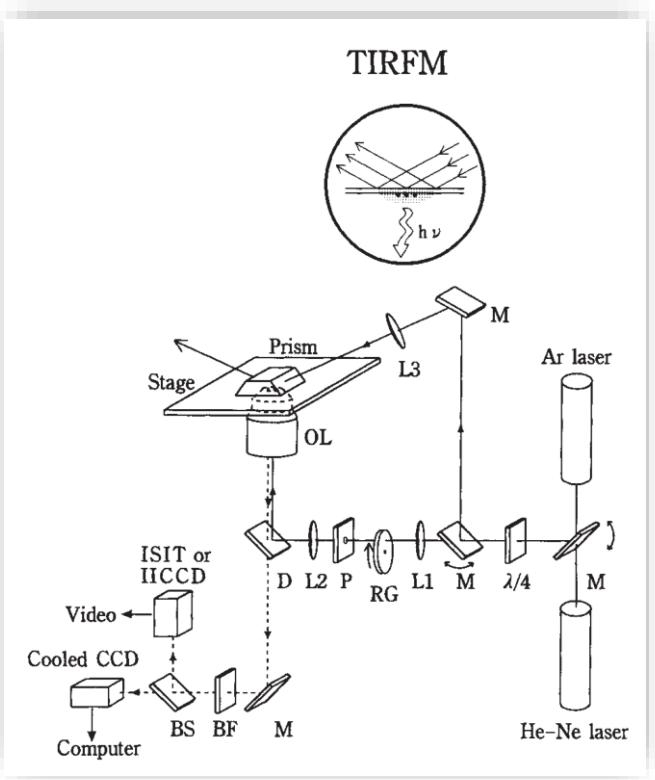

reflection fluorescence microscopy (TIRFM): the laser beam was incident on a quartz microscope slide through a 60° dispersion prism. The gap between the microscope slide and prism was filled with fluorescence-less pure glycerol. Incident angle at the quartz slide-to-solution interface was 68° to the normal (the critical angle is 66°). The beam was focused by a lens (L3) to be 100 μm × 200 μm at the specimen plane. Imaging and analysis: a cooled CCD camera (Series 4200; Astromed, UK) was used for quantitative analysis of the fluorescence intensity with low temporal resolution. For observation of rapid movement or changes in fluorescence intensity, an IICCD camera (C2400-87, Hamamatsu Photonics, Japan) or ISIT camera (C2400-08 and C2400-80H, Hamamatsu Photonics) was used.

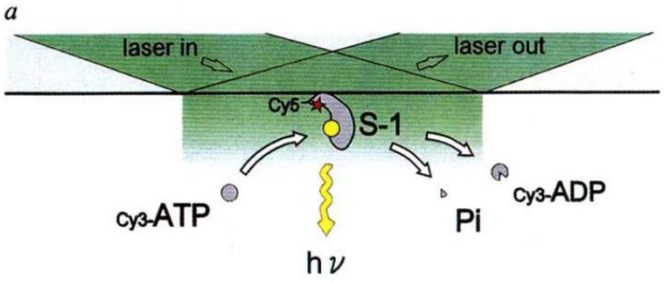

Cy5 myosin S1
670 nm, 5 mW He-Ne

Cy3 nucleotide
570 nm 3.8 mW Ar

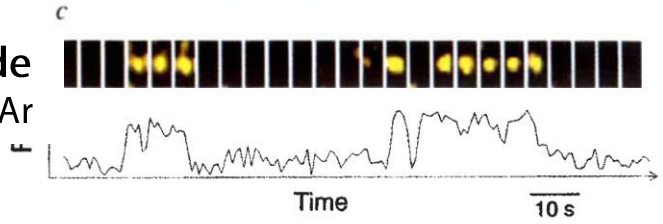

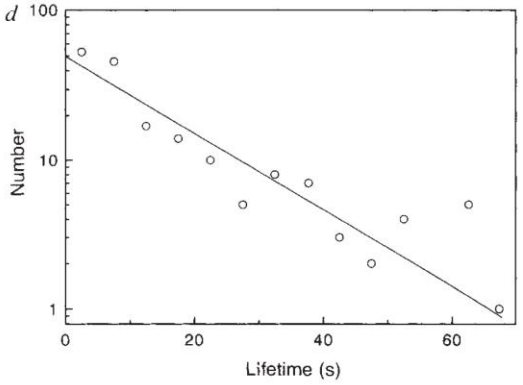

Funatsu et al. Imaging of single fluorescent molecules and individual ATP turnovers by single myosin molecules in aqueous solution. Nature 1995

SINGLE MOLECULE LOCALIZATION MICROSCOPY

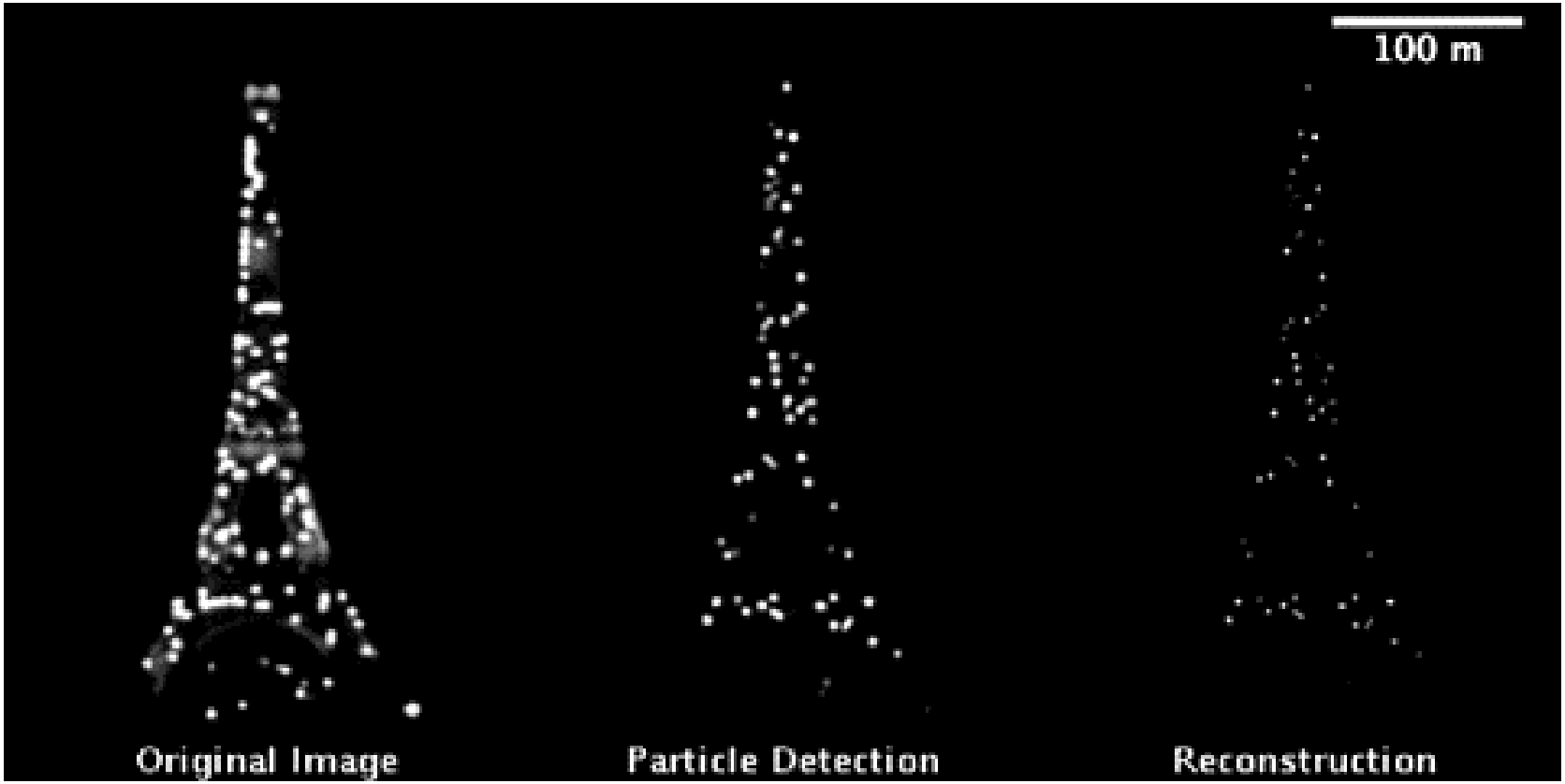

PHOTOTRANSFORMABLE FLUOROPHORES

STANDARD

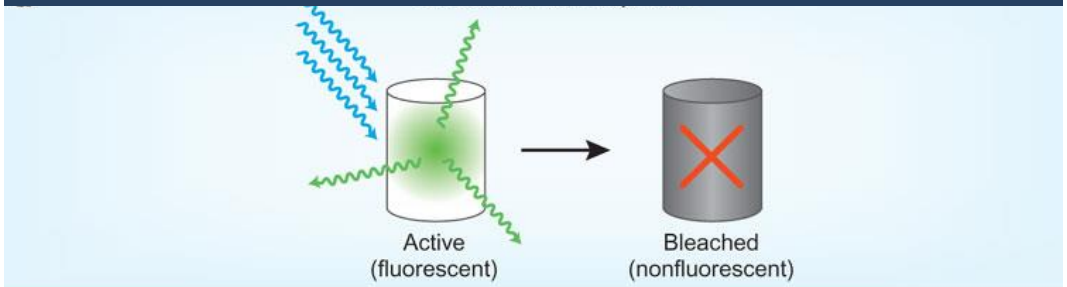

PHOTOACTIVABLE

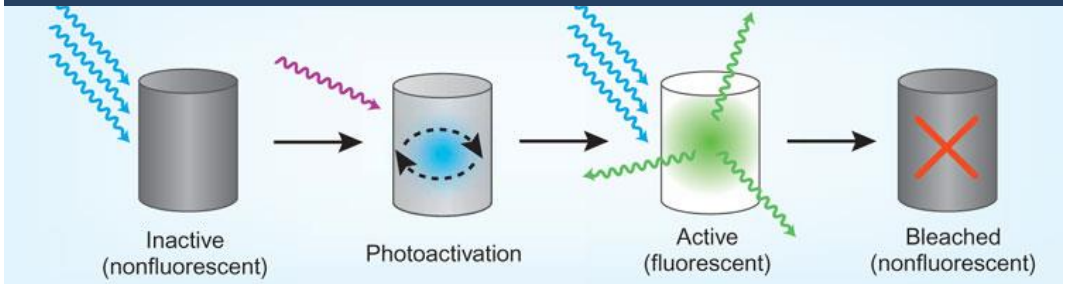

PHOTOCONVERTIBLE

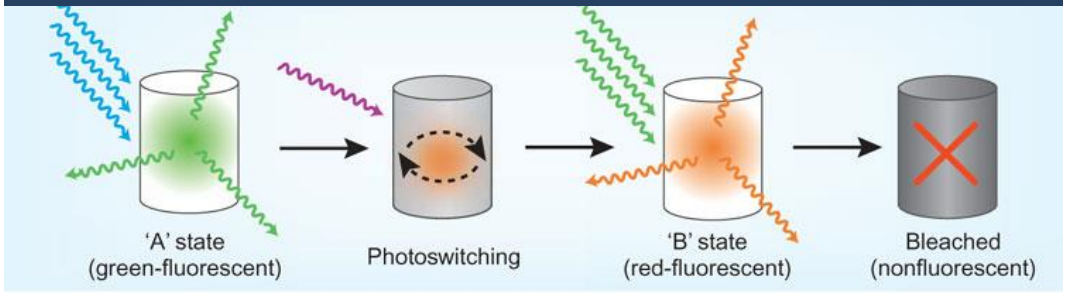

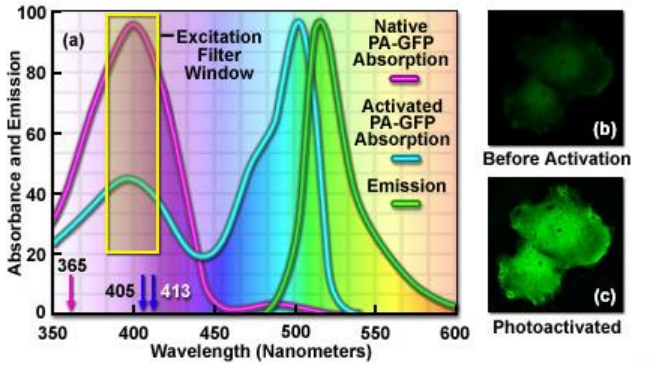

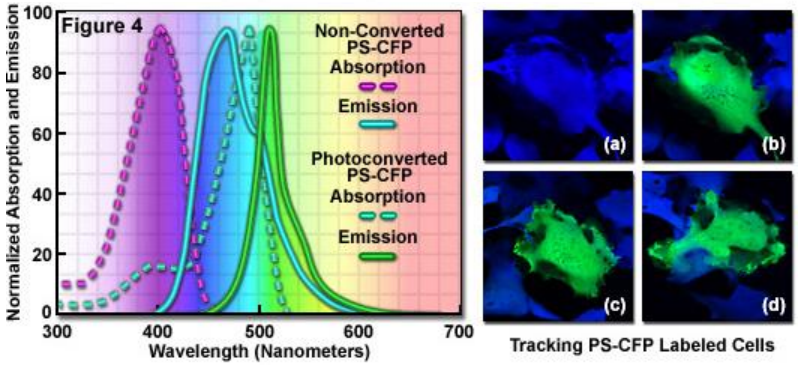

http://www.olympusfluoview.com/applications/opticalhighlighters.html

SINGLE MOLECULE LOCALIZATION MICROSCOPY

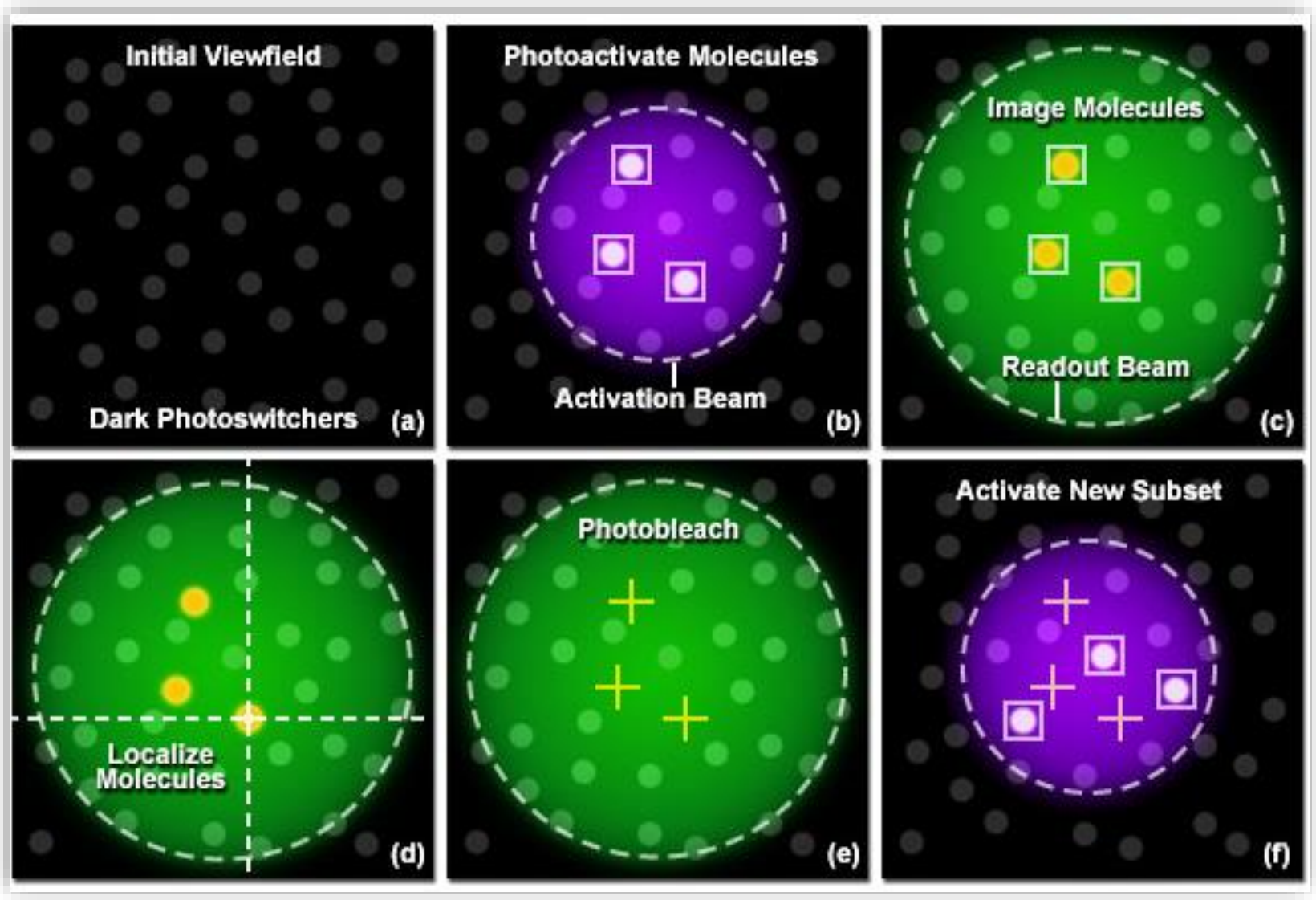

http://zeiss-campus.magnet.fsu.edu/tutorials/superresolution/palmbasics/indexflash.html

SINGLE MOLECULE LOCALIZATION MICROSCOPY

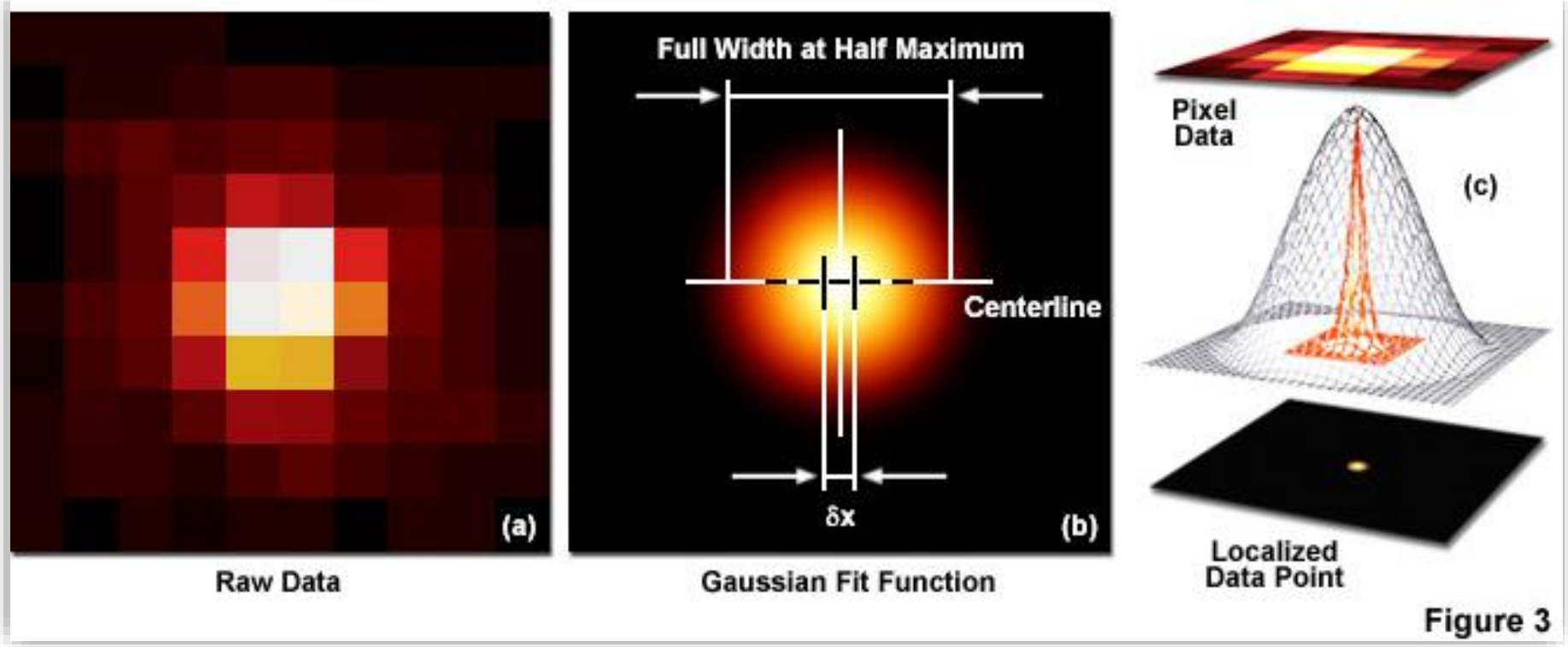

STANDARD ERROR OF PSF ESTIMATION: $\approx \frac{1}{\sqrt{N}} \frac{\lambda}{2nsin\alpha}$

N is the number of photons captured from the fluorescent molecule

http://www.microscopyu.com/articles/superresolution/stormintro.html

SINGLE MOLECULE LOCALIZATION MICROSCOPY

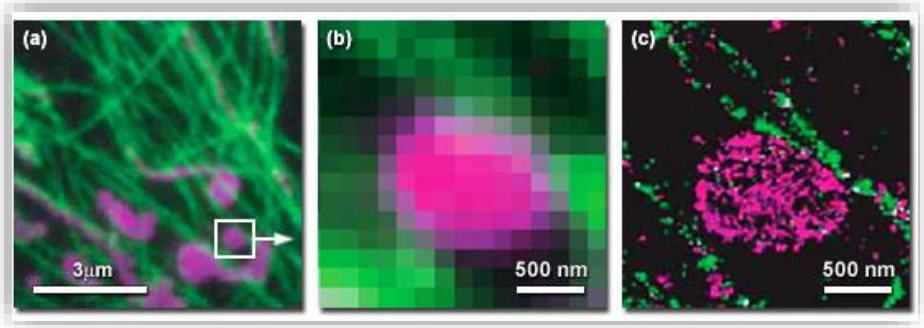

African green monkey kidney cells immunostained with
Alexa Fluor 405 and Cy5: mitochondria
Alexa Fluor 488 and Cy5: microtubule network
activation: 405 nm, 532 nm
readout: 657 nm

Properties of Selected Synthetic Probes for STORM Imaging

Name (Acronym)	Ex (nm)	Em (nm)	EC ($\times 10^{-3}$)	QY	N Photons
Cy3B	559	570	130.0	0.67	1400
Cy3.5	581	596	150.0	0.67	5000
Cy5	649	664	250.0	0.28	4000
Cy5.5	675	694	190.0	0.23	6000
Cy7	747	767	200.0	0.28	1000
Alexa Fluor 488	495	519	71.0	0.92	1200
Alexa Fluor 568	578	603	91.3	0.69	2800
Alexa Fluor 647	650	665	240.0	0.33	6000
Alexa Fluor 750	749	775	240.0	0.12	450
ATTO 488	501	523	90.0	0.80	1300
ATTO 520	516	538	110.0	0.90	1200
ATTO 565	563	592	120.0	0.90	20000
ATTO 647	645	669	120.0	0.20	1500
ATTO 647N	644	669	150.0	0.65	3000
ATTO 680	680	700	125.0	0.3	1500
ATTO 740	740	764	120.0	0.1	1000
TAMRA	546	575	90.4	0.2	5000
Dyomics 654	654	675	220.0	NA	3600
DyLight 750	752	778	220.0	NA	700
IRDye 800 CW	778	794	240.0	NA	3000
Rhodamine B	530	620	105.0	0.65	750
C-Rhodamine	545	575	90.0	0.90	1000
C-Fluorescein	494	518	29.0	0.93	1500

Table 1

http://www.microscopyu.com/articles/superresolution/stormintro.html

STORM OF INDIVIDUAL ACTIN FILAMENTS

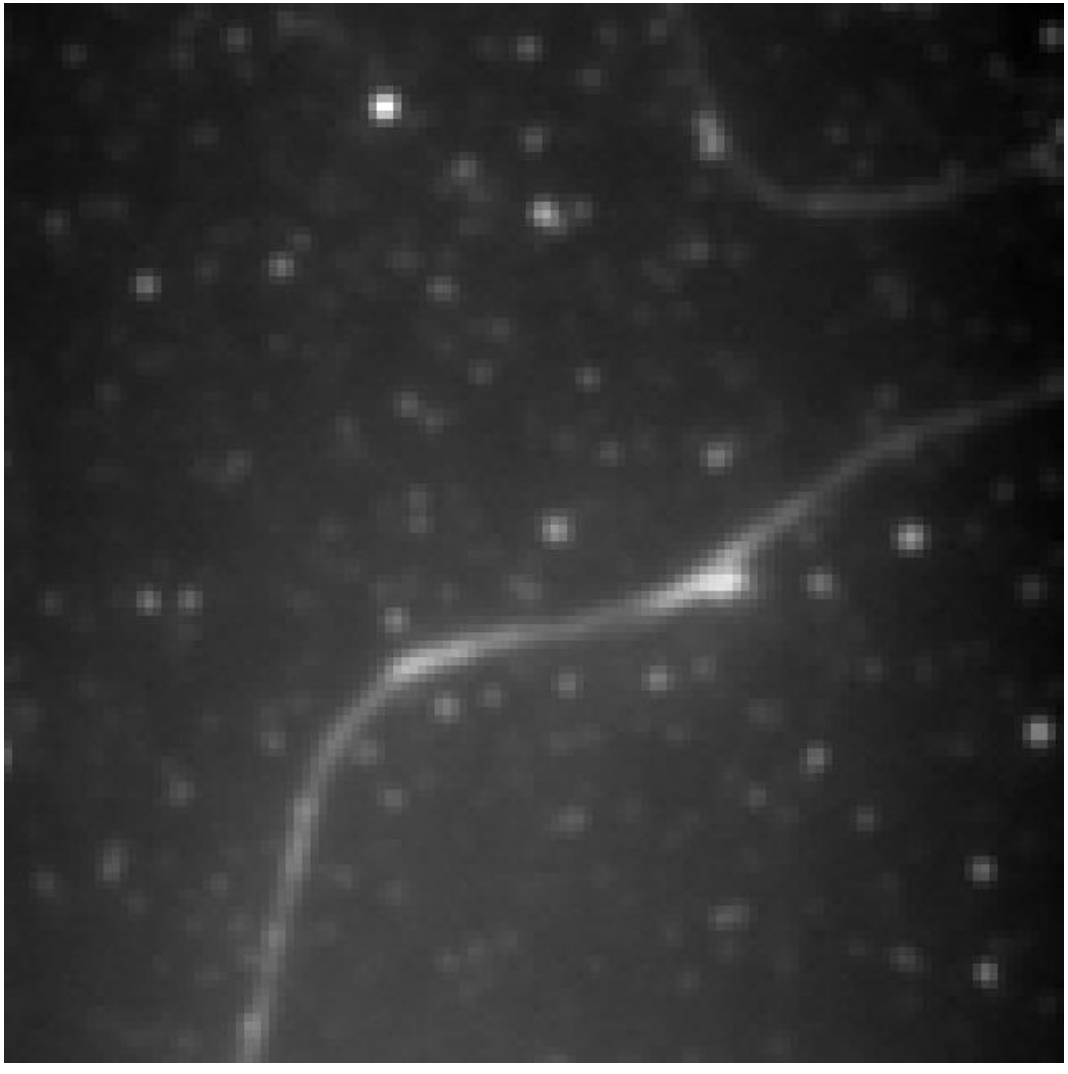

SINGLE MOLECULE LOCALIZATION MICROSCOPY

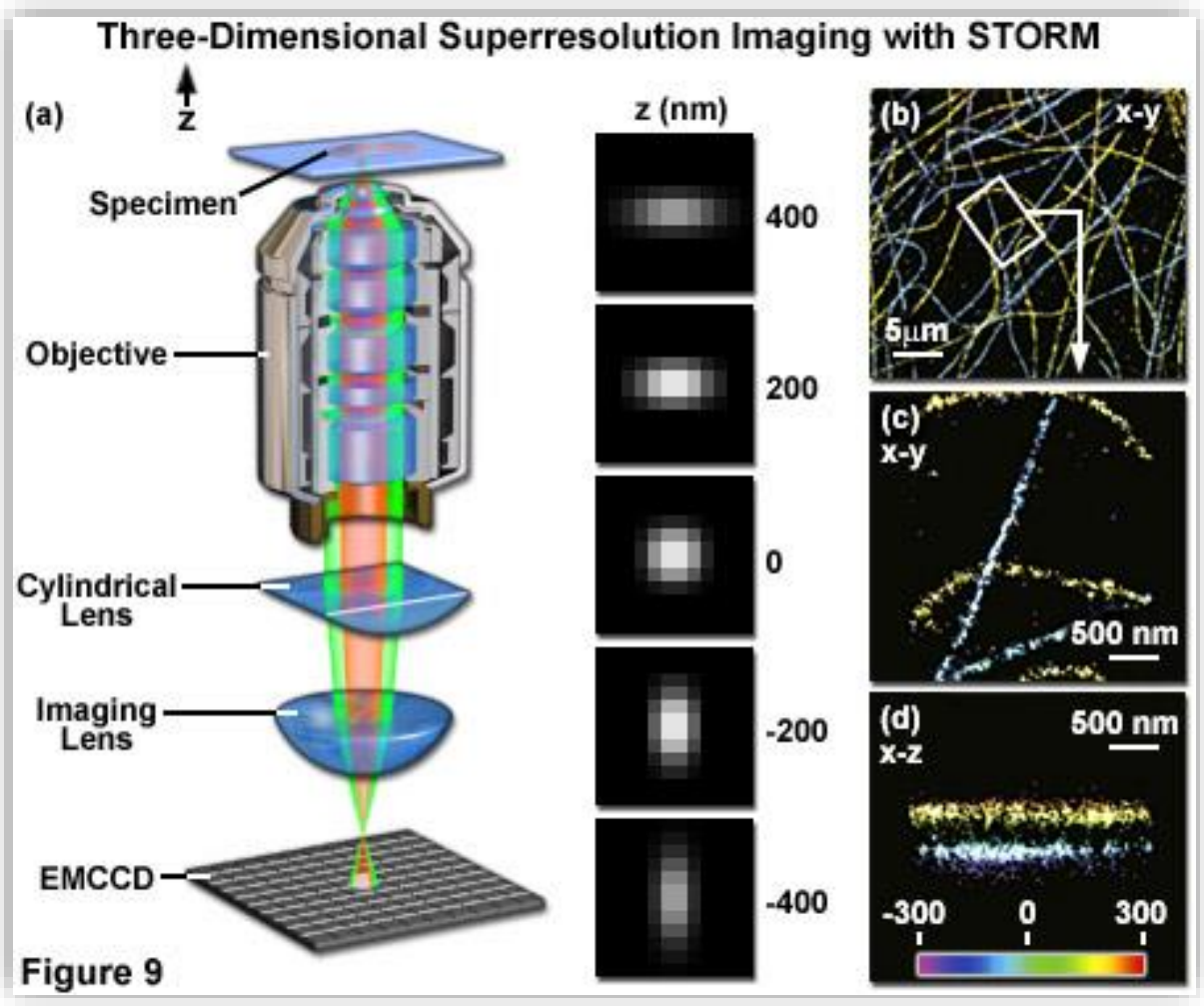

http://www.microscopyu.com/articles/superresolution/stormintro.html

Actin, spectrin and associated proteins form a periodic cytoskeletal structure in axons

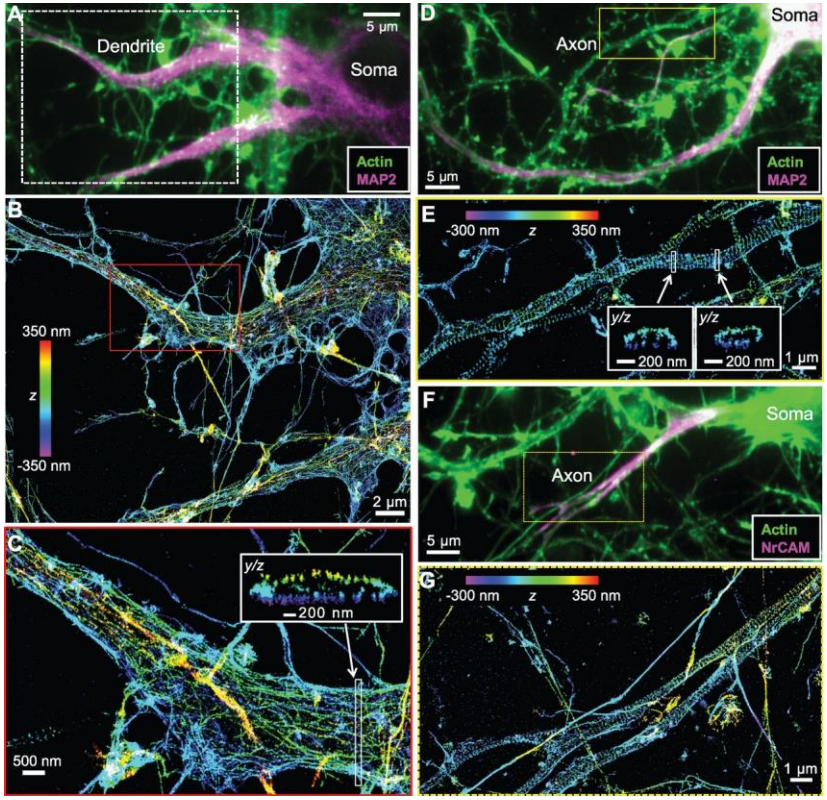

STORM imaging reveals distinct organization of actin filaments in neurons.
axons: rings composed of short actin filaments
dendrites: long actin filaments running along dendritic shafts

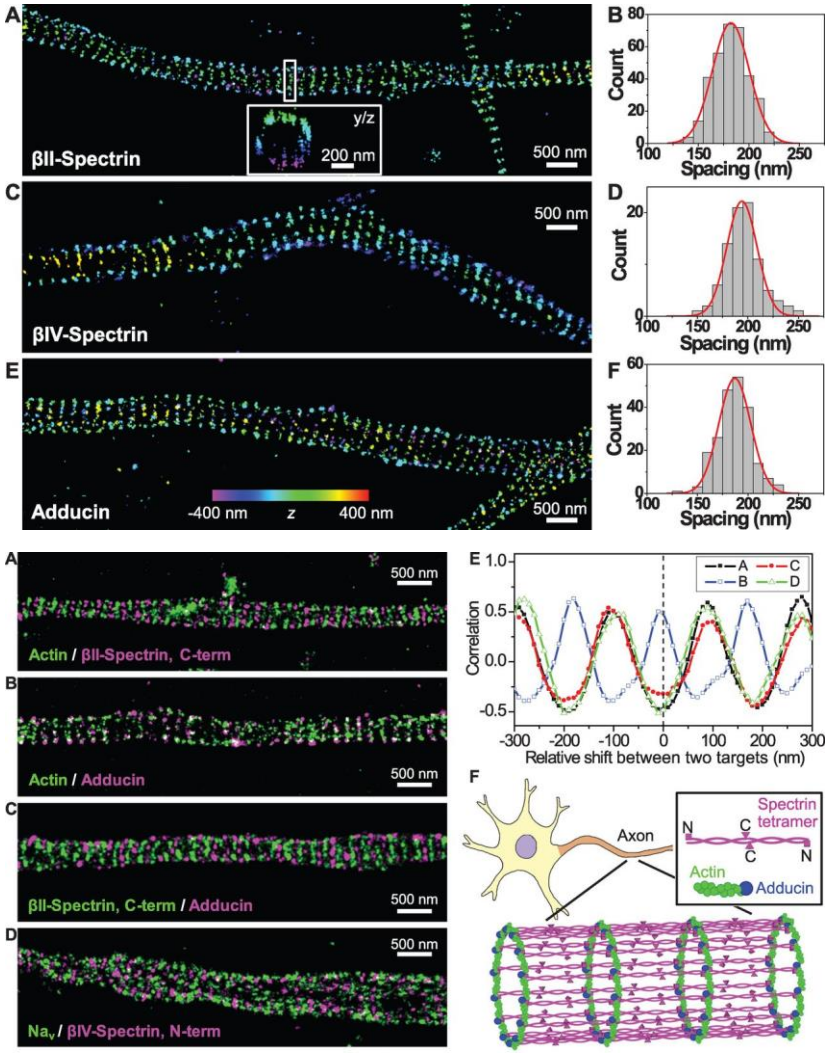

actin – bIIspectrin C terminus [(A), black]
actin - adducin [(B), blue]
adducin - bII-spectrin C terminus [(C), red]
sodium channels - bIV-spectrin N terminus [(D), green]

Zhuang et al. Science 2013

Actin structures in axons – revelaed by Structured Illumination Microscopy (SIM)

Zeiss Elyra SIM, Szentágothai Research Centre, Pécs

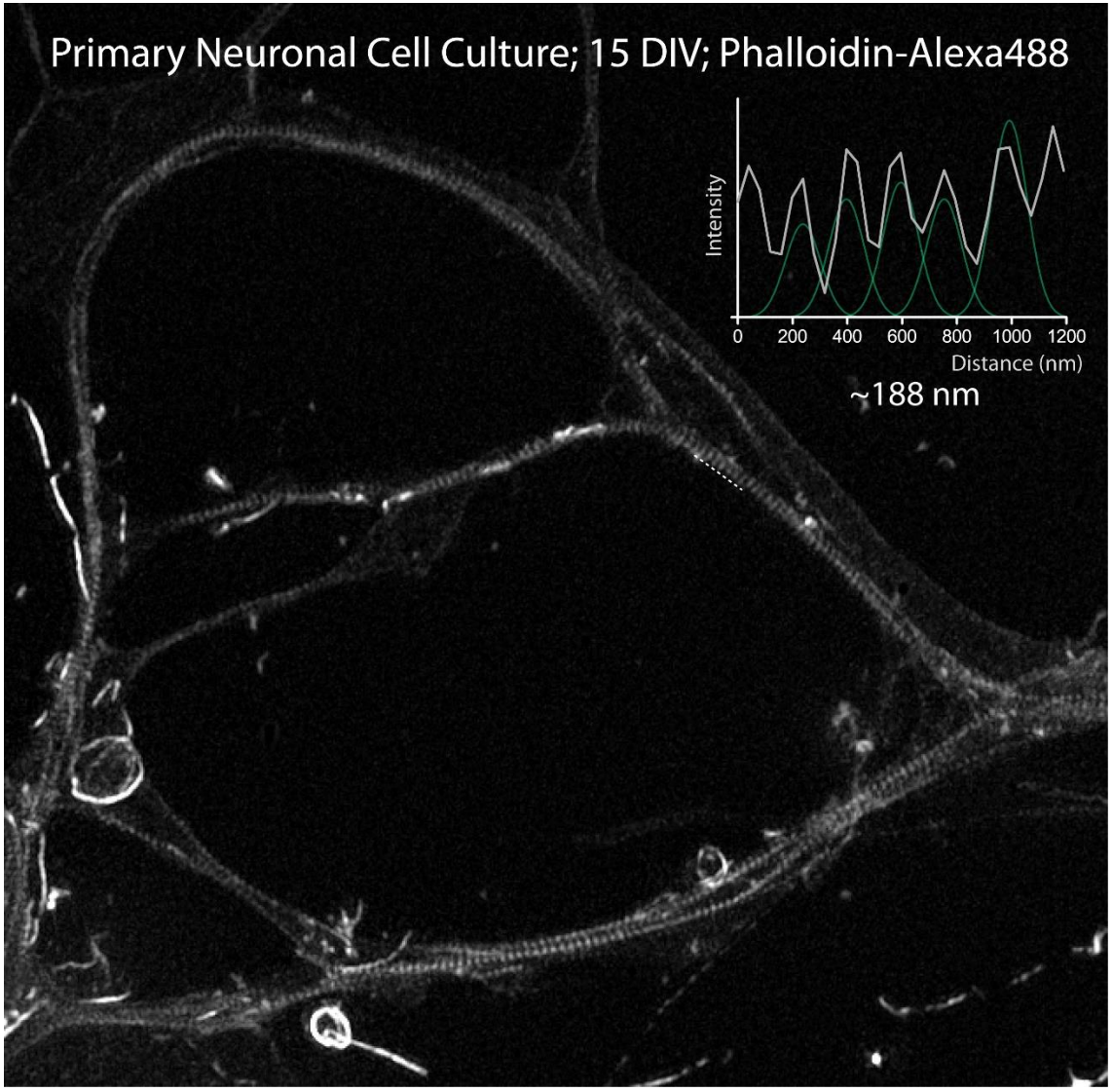

SUMMARY

TIRFM

A NEAR-FIELD IMAGING TECHNIQUE, WHICH PROVIDES SURFACE-SELECTIVE ILLUMINATION DUE TO THE UNIQUE PROPERTIES OF THE EVANESCENT FIELD

PROVIDES RESOLUTION IMPROVEMENT (~100 nm)

USED IN CELL BIOLOGY, PROTEIN BIOCHEMISTRY STUDIES
low phototoxicity, no special fluorophores

CAN BE ADAPTED AND COMBINED WITH OTHER TECHNIQUES

CYTOSKELETAL DYNAMICS GROUP

University of Pécs - Medical School
Department of Biophysics

http://cytoskeletaldynamics.wix.com/mysite

POST DOCS
Tamás Huber
PHD STUDENTS
Andrea Vig
Mónika Tóth
Veronika Kollár
UNDERGRADUATE STUDENTS
Péter Gaszler
Judit Fórizs

Cytoskeleton Dynamics and Motility Group
Laboratoire d'Ezymologie et Biochemie Structurales
CNRS
Gif-sur-Yvette, France

THANK YOU FOR YOUR ATTENTION!